

## REVIEW

Received 00th January  
20xx,Accepted 00th January  
20xx

# Supramolecular Dendrimer-containing Layer-by-Layer Nanoassemblies for Bioapplications: Current Status and Future Prospects

Cristiana F. V. Sousa,<sup>a</sup> Eduardo Fernandez-Megia,<sup>b</sup> João Borges\*<sup>a</sup> and João F. Mano\*<sup>a</sup>

DOI: 10.1039/x0xx00000x

Dendrimers are powerful synthetic macromolecular architectures for a wide variety of bioapplications owing to their unique and superior features, including monodispersity, well-defined and highly branched architecture, multivalency, tunable size and shape, good water solubility, bioavailability, and precisely controllable size at the nanometer-scale. However, the cationic and higher generation dendrimers have generally proven to raise cytotoxicity concerns, which leads to the disruption of cell membranes and cell death, thus extensively limiting their use. Hence, the chemical functionalization of dendrimers' surface with desired functional moieties and their incorporation within supramolecular Layer-by-Layer (LbL) assemblies has been reported as an effective strategy to circumvent the safety issues and improve their biological performance. Herein, we systematically review the multitude of intermolecular interactions behind the build-up of supramolecular dendrimer-containing multifunctional LbL nanoensembles with improved properties and enhanced functionalities for being used in a wide variety of bioapplications. We envisage that such diversity of intermolecular interactions may increase the number of building blocks that can be combined with dendrimers and processed into robust supramolecular multifunctional nanoarchitectures across multiple length scales well-suited to be applied in biological and biomedical scenarios, including in controlled drug/therapeutics/nucleic acid delivery, gene therapy, biosensing, bioimaging, and tissue engineering and regenerative medicine. The review also provides a glimpse on the integration of the bottom-up LbL assembly technology with other bottom-up or top-down approaches for shaping increasingly complex and sophisticated dendrimer-based supramolecular multifunctional devices with high capability for being translated into practical bioapplications.

## 1. Introduction

Dendrimers are powerful synthetic macromolecules that find broad applicability in a wide array of fields owing to their unique and superior structural and physicochemical properties. Those include their monodisperse nature and well-defined hyperbranched three-dimensional polymeric globular architecture, multivalency assigned by the high density of terminal functional groups, high surface area, as well as their tunable nanosize, shape, topology, chemical composition and molecular weight.<sup>1–4</sup> In addition, dendrimers can be designed to denote good water solubility, non-immunogenicity, as well as high biocompatibility, which turn them into highly appealing macromolecules for a wide variety of bioapplications (Fig. 1).<sup>5–13</sup> Those include drug/gene/therapeutics delivery<sup>14–23</sup> and intracellular trafficking,<sup>24–27</sup> gene therapy,<sup>28–30</sup> gene transfection,<sup>31</sup> cancer therapy,<sup>32–34</sup> (bio)molecular imaging,<sup>17,35–41</sup> biosensing,<sup>9,26,42–45</sup> and tissue engineering and regenerative

medicine<sup>16,46–51</sup> due to their intrinsic ability to encapsulate, protect, transport and on-demand targeted release of therapeutic molecules or imaging moieties at desired sites, as well as intrinsic capacity to overcome the extra and intracellular biological barriers.<sup>8,52–59</sup>

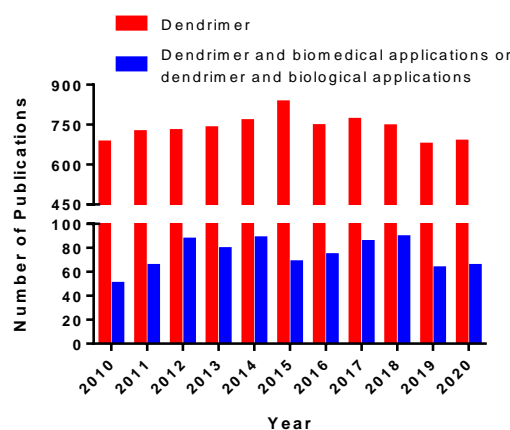


**Fig. 1** Histogram denoting the evolution in the number of yearly publications in the last ten years on the topics “dendrimer”, and “dendrimer and biomedical applications” or “dendrimer and biological applications” in the Web of Science database.

However, most commonly used dendrimers raise cytotoxicity concerns, which extensively limit their practical use in the biological systems.<sup>60</sup> This is particularly notorious for the widely used amine-

<sup>a</sup> CICECO – Aveiro Institute of Materials, Department of Chemistry, University of Aveiro, Campus Universitário de Santiago, 3810-193 Aveiro, Portugal  
E-mail: joaoborges@ua.pt (J.B.), jmano@ua.pt (J.F.M.)

<sup>b</sup> Centro Singular de Investigación en Química Biolóxica e Materiais Moleculares (CIQUS) and Departamento de Química Orgánica, Universidade de Santiago de Compostela, 15782 Santiago de Compostela, Spain

ended dendrimers of higher generations (usually  $G \geq 4$ ), including poly(amidoamine) (PAMAM), poly(ethylene imine) (PEI), poly(propylene imine) (PPI), and poly(L-lysine),<sup>48,61–63</sup> due to their multiple surface cationic charge and high propensity to interact and disrupt the cell membrane and lead to cell death. To improve the biological functionality and, thus, performance of the cationic dendrimers under physiological conditions, considerable efforts have been made on the peripheral functionalization of their amine end groups with poly(ethylene glycol) (PEG),<sup>18</sup> or through conjugation with natural saccharides<sup>64</sup> or other targeting-specific ligands or cargoes.<sup>13,19,21</sup> Besides, the rational design and development of dendrimer-containing multifunctional multilayered assemblies,<sup>65</sup> by resorting to the prominent LbL assembly technology, has been also deemed as a powerful strategy to mitigate their cytotoxicity owing to its key enabling features. The LbL technology, firstly introduced by Iler in 1966<sup>66</sup> and mostly known after the seminal work by Decher and co-workers in the 1990s,<sup>67–71</sup> has quickly emerged as a simple, cost-effective, efficient, and highly versatile bottom-up methodology to functionalize surfaces and precisely assemble robust and conformal multilayered architectures, under mild conditions, with finely tuned compositions, structures, properties and functions at the nanoscale.<sup>72</sup> Such versatility is illustrated by the multitude of templates,<sup>73,74</sup> assembly methodologies,<sup>75–82</sup> and intermolecular interactions<sup>83</sup> that enable the precise, controlled and elegant nanoscopic assembly of an unprecedented array of complementary building blocks into a diverse set of advanced functional multidimensional LbL architectures with applications in a myriad of fields (Fig. 2).<sup>81,83–101</sup> To date, the LbL technology has been by far mostly widely employed to assemble oppositely charged polymers by resorting to attractive electrostatic interactions.<sup>69,71,83,87,100</sup> Among them, dendrimers are very promising building blocks to be used as ingredients within LbL assemblies owing to their unique features and high versatility.

biological activity of therapeutic agents until they are administered and delivered at desired locations is a key feature of the LbL assembly technology.<sup>96,102–104</sup> Therefore, dendrimer-containing LbL nanoassemblies represent prominent platforms for a wide array of bioapplications, overcoming the limitations associated with the employment of free dendrimers.<sup>105,106</sup> Moreover, in contrast to the multilayered systems enclosing linear polymers, the dendrimer-containing LbL assemblies have shown that dendrimers can penetrate into the interlayers. Although the thickness, morphology and growth of the multilayers are strongly influenced by the assembling conditions, the strong interactions between dendritic polymers and the substrate make dendrimers able to change their conformation to increase the adsorption point. Furthermore, the employment of dendrimers has shown to be highly advantageous to obtain thicker films.<sup>107</sup>

In this review, we systematically overview the multitude of intermolecular interactions behind the fabrication of supramolecular dendrimer-based multilayered assemblies using the LbL assembly technology to be used in a wide array of bioapplications, including biosensing, drug/therapeutics delivery, and gene therapy. Several examples are given on supramolecular dendrimer-containing multilayered nanoensembles fabricated from electrostatic, host-guest, coordination chemistry, and biologically specific interactions, as well as from hydrogen bonding, and covalent bonding. Moreover, the potential impact of the developed supramolecular LbL nanoassemblies in biomedical and biological applications is also discussed. The last section provides a glimpse on the current status and future perspectives on the integration of dendrimers and LbL assembly technology with either other bottom-up and/or top-down methodologies aiming for the rational design and development of complex and innovative supramolecular nanodevices, exhibiting improved properties and enhanced multifunctionalities, for being used in a wide array of biomedical, biological and biotechnological applications.

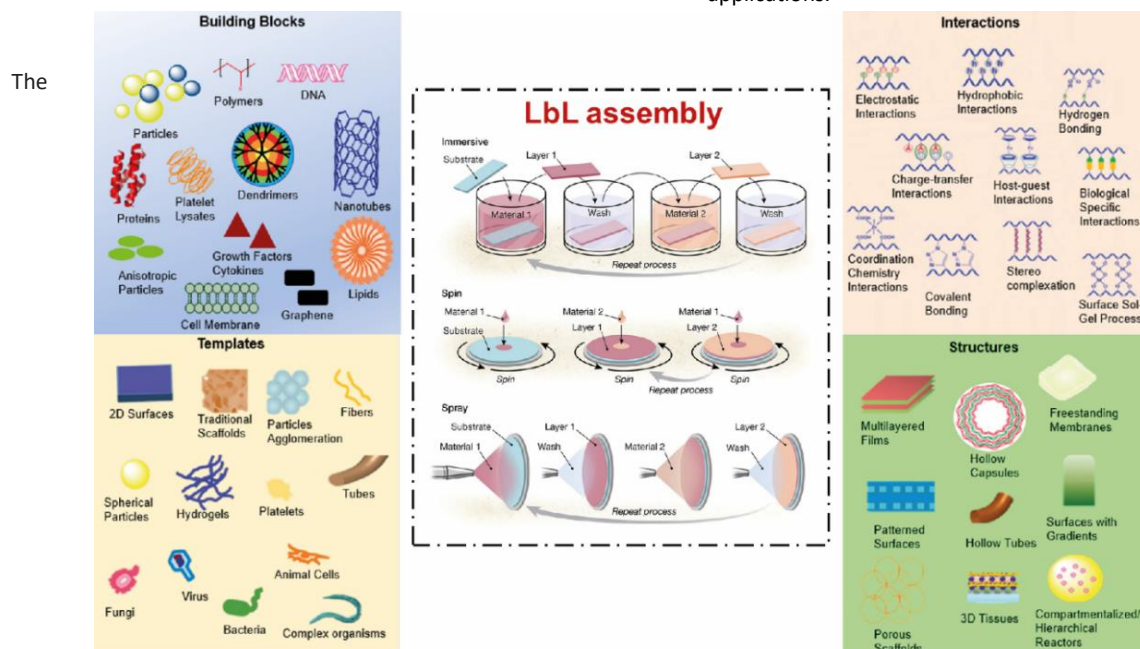


**Fig. 2** Schematic illustration of high versatility endowed by the LbL assembly technology. The final properties, functions, performance and end-used of the resulting multilayered structures are intrinsically dependent on the template features, building blocks, intermolecular interactions, and assembly methodologies. Adapted from ref. 81 with permission from the American Association for the Advancement of Science. Adapted from ref. 97 with permission from the Wiley-VCH Verlag GmbH & Co.

ability of the LbL ensembles to encapsulate, protect and preserve the

## 2. Driving forces behind the fabrication of dendrimer-containing LbL assemblies

### 2.1 Electrostatic interactions

The electrostatic interaction is the most explored mechanism behind the fabrication of multilayered assemblies when both the molecule and the adsorbent surface are electrically charged.<sup>83,108</sup> Recently, considerable attention has been devoted to the combined use of dendrimers and oppositely charged polymers (Fig. 3a) or solely oppositely charged dendrimers (Fig. 3b) as building blocks for the development of electrostatically-driven supramolecular multilayered thin films taking advantage of their charged terminal functional groups, such as amine, carboxyl, or sulfate groups.<sup>109–116</sup> This intermolecular interaction represents the most explored method to prepare multilayered assemblies encompassing dendrimers.

generations on a silicon wafer.<sup>119</sup> The authors assembled up to 20 layers and demonstrated that the PAMAM dendrimers were highly compressed and flattened. Moreover, Yoshimura and co-workers developed LbL films containing dendrimers surface functionalized with oppositely charged metal nanoparticles (NPs), namely oppositely charged gold (Au)- and silver (Ag)-dendrimer nanocomposites for being used as thin conducting or catalytic films.<sup>120</sup> It has been demonstrated that several physicochemical parameters, including the solution pH and ionic strength and the intrinsic properties of the polyelectrolytes such as the concentration, molecular weight and charge density play a key role in the deposition, stability, structure, properties and functions of the assembled multilayered structures, as described below.<sup>83,121</sup>

#### 2.1.1 Factors governing the growth of LbL assemblies

##### 2.1.1.1 Influence of solution pH

Many dendritic families include tertiary amines at the interior and

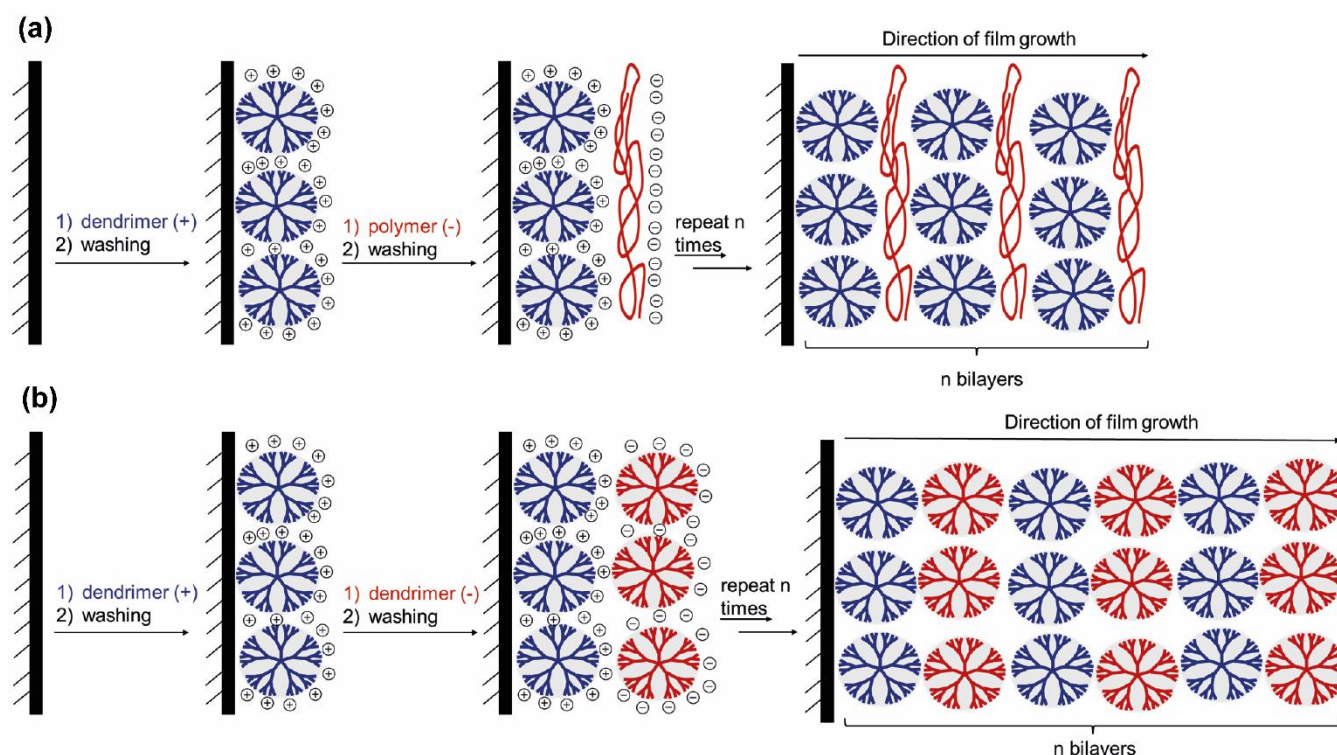


**Fig. 3** Schematic illustration denoting the preparation of (a) dendrimer/polymer and (b) dendrimer/dendrimer LbL nanofilms on solid surfaces via electrostatic interactions. In-between the alternate immersion in the polycation and polyanion aqueous solutions, the substrate is immersed in an aqueous solution to remove weakly adsorbed layers and avoid the contamination of the polymer solutions by liquid adhering to the substrate.

Indeed, LbL films encompassing dendrimers and distinct oppositely charged polymers, such as carboxylated azopolymer,<sup>109,114</sup> poly(acrylic acid) (PAA),<sup>110</sup> sulfonated poly(aniline) (SPANI),<sup>111</sup> polyaniline (PANI),<sup>117</sup> poly(styrene sulfonate) (PSS),<sup>115</sup> poly(vinyl sulfonic acid) (PVS),<sup>112</sup> poly(diallyl-dimethylammonium chloride) (PDDA) and carboxylated poly(glycerol)<sup>113</sup> have been developed. Among the dendrimers, PAMAM has been the most widely used to build-up multilayered structures due to their straightforward synthesis, low polydispersity and commercial availability.<sup>118</sup> Besides the fabrication of dendrimer/polymer multilayered assemblies, similar LbL systems have been also developed by resorting to solely oppositely charged dendrimers. In this regard, Tsukruk *et al.* reported the build-up of multilayered films comprising amine- and carboxyl-terminated PAMAM dendrimers of adjacent

primary amines on the surface and, as such, their conformation in aqueous solution is affected by changes in the pH, which in turn influence the preparation of dendrimer-based LbL films assembled via electrostatic interactions.<sup>106,107</sup> The  $pK_a$  of terminal primary amines is 9.23 whereas the  $pK_a$  of tertiary ones at the branching points is 6.3.<sup>122</sup> In this regard, at high pH, dendrimers denote a denser and globular conformation with lower surface charge density because only the primary amines on the terminals are protonated. In contrast, at low pH, dendrimers with an open and extended conformation and higher charge density prevail due to the repulsions between the protonated tertiary amines at the interior and primary amines at the surface.<sup>111</sup> In fact, Kim and Bruening revealed that the PAMAM/PAA multilayered growth is dependent on the solution pH.<sup>110</sup> The highest thickness was obtained while assembling PAMAM

and PAA aqueous solutions at pH 8 and 4 (Fig. 4a,b), respectively, since both PAMAM and PAA are only partially charged. Moreover, those films exhibited the highest surface roughness, which is probably assigned to the fastest formation of the film (Fig. 4c-f). Almost at the same time, Imae and co-workers prepared SPANI/PAMAM LbL films and investigated the influence of the solution pH on the film growth.<sup>111</sup> They assembled multilayered films composed of either SPANI and PAMAM solutions at pH 6 (fully charged) or PAMAM at pH 9.8 (partially charged) and SPANI at pH 6 (fully charged) and found that the amount of SPANI and PAMAM adsorbed during the multilayered film growth using PAMAM solutions at pH 9.8 is larger than the one adsorbed while resorting to solutions at pH 6 due to the lower surface charge and more condensed structured denoted by PAMAM, which reduces the layer interpenetration and leads to a highly ordered multilayered film. It was also shown that, irrespectively of the pH of the solutions, the amount of SPANI and PAMAM adsorbed increased while increasing the number of bilayers.

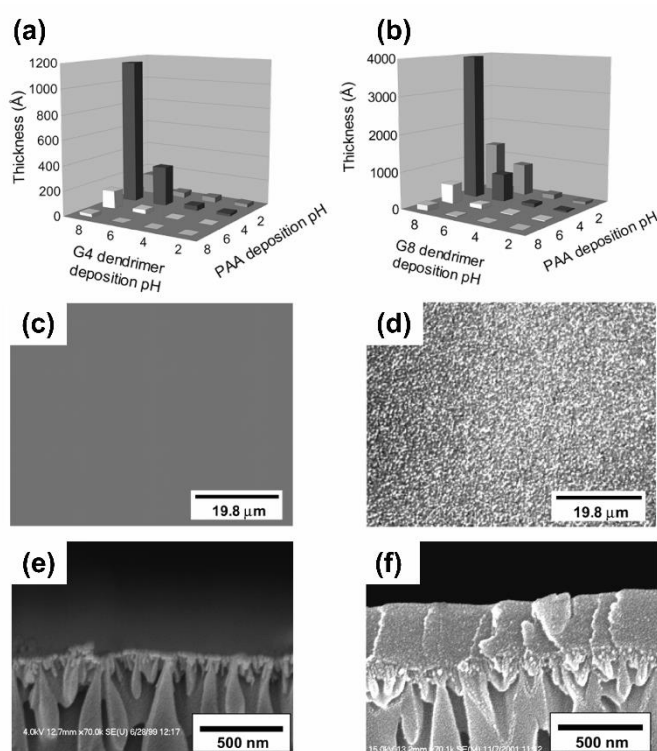


**Fig. 4** Influence of the solution pH in the thickness of 2.5 bilayers composed of (a) G4 PAMAM dendrimers and PAA and (b) G8 PAMAM dendrimers and PAA. Microscopy images of 2.5 bilayers of (c) G8 PAMAM (pH = 4) and PAA (pH = 4) and (d) G8 PAMAM (pH = 8) and PAA (pH = 4). The ellipsometric thickness of the films were 80 and 4000 Å, respectively. Scanning electron microscope (SEM) images of the cross section of porous alumina (e) before and (f) after coating with 4.5 bilayers of G4 PAMAM (pH = 8) and PAA (pH = 4) film. Adapted from ref. 110 with permission from the American Chemical Society.

### 2.1.1.2 Influence of ionic strength

The growth of multilayered films is also strongly influenced by the ionic strength. In this regard, Li *et al.* reported that, at high ionic strength (0.4 M), charged dendrimers display a denser core conformation (Fig. 5a) with a lower surface charge whereas at low ionic strength (0.2 M), dendrimers exhibited higher charge density and might adopt a disk-like structure (Fig. 5b) and, as such, more

dendritic molecules will be absorbed into the film surface because of the balance of the charges.<sup>111</sup> Moreover, the addition of salt increased the adsorption of SPANI in SPANI/PAMAM LbL films (Fig. 5c), which can be due to the partially neutralization of its net charge. Khopade and Caruso also studied the influence of salt concentration in the growth of multilayered films encompassing PAMAM and PSS, showcasing that the amount of adsorbed PSS per bilayer increased while increasing the salt concentration up to 0.5–1 M, after which it started to decrease to values similar to the ones obtained in the absence of salt (Fig. 5d).<sup>123</sup>

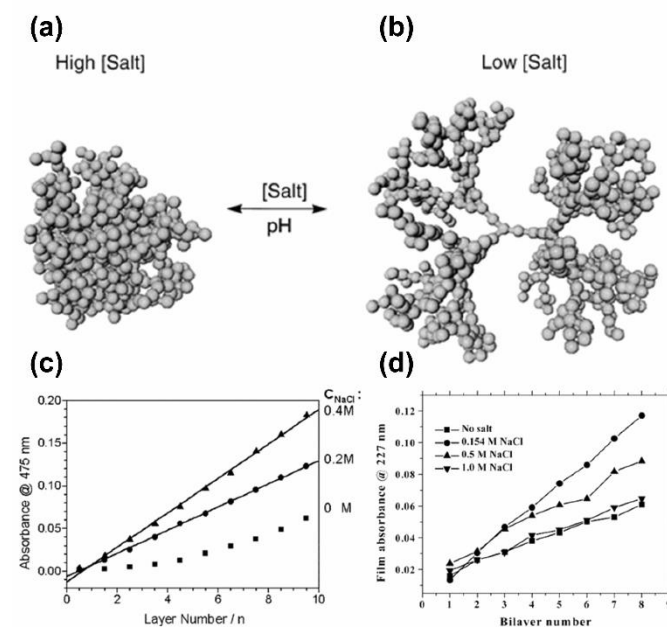


**Fig. 5** Schematic illustration of analogous dendrimers to G6 PAMAM in the presence of (a) high salt and (b) low salt concentration. Reprinted from ref. 124 with permission from the American Chemical Society. (c) Effect of the ionic strength on the absorbance at 475 nm in SPANI/PAMAM multilayered films as a function of the number of layers. Reprinted from ref. 111 with permission from the American Chemical Society. (d) Evolution of the absorbance at 227 nm as a function of the number of deposited bilayers for PSS/PAMAM multilayered films prepared in buffer containing different salt concentrations. The substrate was coated with a priming layer of PEI solution, followed by alternating layers of PSS and PAMAM via electrostatic interactions. Adapted from ref. 123 with permission from the American Chemical Society.

Almost fifty years ago, van den Berg and Staverman suggested the formation of PEI-anionic surfactant sodium dodecyl sulfate (SDS) complexes by the association of PEI, SDS and sodium chloride (NaCl).<sup>125</sup> Later on, Windsor *et al.* showed that the addition of NaCl to PEI containing solutions at a low ionic strength induced a large ordering effect on adsorbed SDS at a lower bulk concentration at the solid-liquid interface, attributing these conformational changes to the formation of a complex between PEI and SDS.<sup>126</sup> In this regard, Wang and co-workers developed multilayered films containing positively charged PEI dendrimer and oppositely charged azobenzene polymer (PAZO)-SDS and evaluated the effect of SDS in the film growth behavior.<sup>127</sup> It was found that the amount of PAZO adsorbed decreased while increasing the concentration of SDS, until the critical micelle concentration of SDS was reached, due to the competition of SDS and PAZO for PEI binding sites. Thus, the adsorption of SDS was followed by a slower PAZO adsorption step, with PAZO occupying the remaining binding sites on the PEI layer. As

such, SDS interpenetrates through the PAZO and PEI layers, which in turn improves the surface hydrophobicity of both.

### 2.1.1.3 Influence of dendrimer generation, polymer molecular weight, concentration and charge density

The effect of the dendrimer generation, polymer molecular weight and material's concentration on the film growth and the architecture of the resulting multilayered films have been also explored. For instance, Khopade and Caruso studied the build-up of multilayered films composed of PAMAM dendrimers bearing terminal primary amines and negatively charged PSS on the quartz crystal microbalance (QCM), which revealed a linear growth of the multilayered film (Fig. 6a). However, the ultraviolet-visible (UV-Vis) spectra of the multilayered film growth showed a partial removal of PSS layers after the deposition of PAMAM, revealing an adsorption-desorption trend (Fig. 6b).<sup>123,128</sup> We hypothesize that the different behavior observed in Fig. 6a and b is assigned to the removal of PSS from the film by the dendrimer solution but may also be a consequence of the PAMAM removal from the film to the PSS solution after the deposition of PSS. Unfortunately, the desorption of PAMAM could not be verified in the UV-Vis spectra because PAMAM does not absorb within the range analyzed. Moreover, it was shown that the multilayered film growth increased linearly while increasing the dendrimer generation (Fig. 6c) or PSS molecular weight (Fig. 6d).

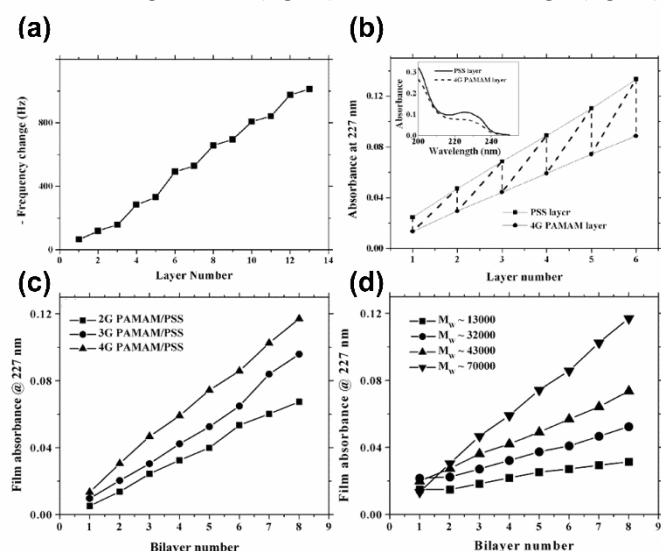


**Fig. 6** (a) QCM frequency shift against layers number of PSS/PAMAM multilayered film. (b) Evolution of the absorbance at 227 nm as function of the number of layers of PSS/PAMAM deposited on a quartz slide. The inset figure shows the UV-Vis spectra after PSS (solid line) and PAMAM dendrimer (dotted line) adsorption. Reprinted from ref. 128 with permission from the American Chemical Society. Evolution of the absorbance at 227 nm in PSS/PAMAM multilayered films, prepared with (c) generation 2, 3 or 4 PAMAM dendrimers and (d) PSS with a molecular weight of 13 000, 32 000, 43 000 or 70 000 Da, as a function of the number of layers. The first layer deposited was PEI, followed by alternate adsorption of layers of PSS and PAMAM. Reprinted from ref. 123 with permission from the American Chemical Society.

Furthermore, LbL films prepared by alternate immersion of glass substrates into solutions of PPI dendrimer with amino surface groups (DAB-Am) and metallic AgNPs revealed that the multilayered film growth was higher with *G5* dendrimers than with the *G1* counterparts (using the same concentration).<sup>129</sup> Such behavior suggests that *G5* dendrimers have more available amino terminal functional groups able to bind AgNPs when compared with the *G1*

dendrimers. Moreover, it was found that the number of deposited layers plays a key role in the morphology and roughness of the multilayered films. Similarly, Mendonça and co-workers developed multilayered films comprising *G1*, 3 or 5 DAB-Am dendrimers and PAZO and observed that the amount of PAZO adsorbed per bilayer was higher when a DAB-Am of higher generation was used.<sup>114</sup> Kim and Bruening also studied the influence of the dendrimer generation and polymer molecular weight by developing LbL films encompassing *G4* or *G8* PAMAM dendrimers and PAA of 2 000 or 90 000 Da and observed that the multilayered film growth was much smaller while resorting to the lower dendrimer generation and PAA with molecular weight of 2 000.<sup>110</sup> Furthermore, the multilayered films developed by Imae and co-workers, comprising SPANI and PAMAM, showed that the amount of SPANI adsorbed per bilayer increased while increasing its concentration until a maximum of ~1 mM and then decreased.<sup>111</sup> As such, when a SPANI solution of high concentration (5 mM) was used, more PAMAM dendrimers adsorbed in the previous layer were removed by the SPANI chains, leading to a decrease in the surface charge density and, therefore, less SPANI adsorbed.

## 2.2 Hydrogen bonding

Although the electrostatic interaction between oppositely charged building blocks is by far the most commonly employed driving force in the build-up of multilayered films, many other intermolecular interactions can be used, enabling the incorporation of uncharged materials within the LbL assemblies. Those interactions include hydrogen bonding,<sup>130,131</sup> which is a feasible driving force to create multilayered films, provided that the building blocks to be assembled present moieties that can act as hydrogen bonding donors and acceptors.<sup>83,132</sup> Hydrogen-bonded LbL films are prepared in a manner reminiscent of electrostatically-driven LbL films, i.e. by the alternate immersion of virtually any type of substrate in solutions of hydrogen donor and acceptor materials.<sup>132</sup> Although the formation of hydrogen-bonded LbL films can be performed in aqueous solutions, which is highly desired when working with biological materials, it can also be attempted in organic solvents, thus enabling the incorporation of water-insoluble materials within the assembly process.<sup>130,131</sup>

### 2.2.1 Hydrogen bonding-based single component films

Dendrimers presenting carboxyl groups on its periphery, thus acting as hydrogen bonding donor, as well as hydrogen bonding acceptor have been used as film components. In this regard, Huo *et al.* reported the build-up of a single component hydrogen-bonded LbL assemblies (Fig. 7a) encompassing solely a carboxyl-terminated polyether dendrimer (DEN-COOH) (Fig. 7b), acting both as hydrogen bonding donor and hydrogen bonding acceptor.<sup>133</sup> Although the dendrimer adsorption process was continuous and uniform during the production of the multilayered film, the infrared reflection and transmission spectra suggest that some rearrangements occurred in the dendrimers after their deposition on the substrate, which may facilitate the formation of hydrogen bonding for stabilizing the multilayers. Two years later, Sun *et al.* also demonstrated that single component multilayered assemblies can be prepared by self-deposition of one or two generations of dendrimers.<sup>134</sup> The authors developed single component multilayered films using either the first (Fig. 7c) or second (Fig. 7d) generation of poly(aryl ether) dendrimers with a diphenylanthracene core, and 8 or 16 carboxyl end groups, named [An(*G1*)<sub>4</sub>] and [An(*G2*)<sub>4</sub>], respectively. It was shown that even the An(*G1*)<sub>4</sub> was able to provide enough hydrogen bonding pairs for the preparation of multilayered films. In both cases, the films presented granular morphology with roughness of 0.254 and 0.457 nm, respectively. The difference in roughness was attributed to the

molecular structure of the dendrimers. This work demonstrated that the multilayered process can be performed using different generations of the same dendritic family (Fig. 7e).

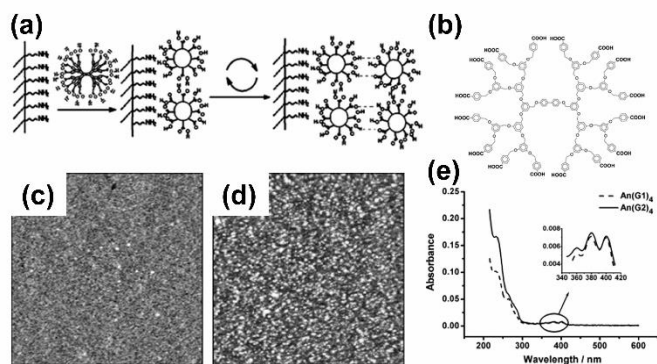


**Fig. 7** (a) Schematic illustration of the LbL assembly process encompassing a single component dendrimer on a  $\text{NH}_2$ -modified quartz substrate via hydrogen bonding. (b) The chemical structure of DEN-COOH. Reprinted from ref. 133 with permission from the Royal Society of Chemistry. Atomic force microscopy (AFM) images of nine bilayers of (c)  $\text{An}(G1)_4$  and (d)  $\text{An}(G2)_4$  assembled on a quartz substrate. The image size is  $1.5 \mu\text{m} \times 1.5 \mu\text{m}$ . (e) UV-Vis absorption spectra of single component films by self-deposition of either  $\text{An}(G1)_4$  or  $\text{An}(G2)_4$  with similar characteristic absorption of diphenylanthracene in the range between 350–410 nm. Adapted from ref. 134 with permission from the Elsevier.

### 2.2.2 Effect of the hydrogen bonding donor architecture on the release rate and structure of multilayered assemblies

A multilayered film relying on two different components was also reported by the alternate deposition of DEN-COOH (hydrogen bonding donor) and poly(4-vinylpyridine) (PVP) (hydrogen bonding acceptor) (Fig. 8a).<sup>130</sup> Surprisingly, DEN-COOH was slowly released from PVP/DEN-COOH multilayered films when compared to the release rate of PAA from PVP/PAA multilayered films, in a basic solution.<sup>135</sup> Those films exhibited different microporous morphology, which in turn prove that the molecular structure of a building block influences the behavior of multilayered films prepared by hydrogen bonding. However, it is important to bear in mind that those differences can also be the result of the different number of assembled layers. As can be seen from Fig. 8b, the immersion of PVP/DEN-COOH multilayered films for 10 min in a basic solution ( $\text{pH} = 12.5$ ) led to a high and homogeneous surface coverage with granular structures, and no porous structure was observed. However, after the immersion for longer times (Fig. 8c–e), the PVP/DEN-COOH multilayered film revealed the formation of nanosized pores with a higher diameter and depth. More recently, Sun *et al.* developed multilayered films by the alternate deposition of mixed solutions of two carboxyl-ended poly(aryl ether) dendrimers [ $\text{Por}(G2)_4$  with porphyrin core and  $\text{An}(G2)_4$  with an diphenylanthracene core] and PVP.<sup>136</sup> It is worth mentioning that the composition of the two dendrimers in the multilayered films can be adjusted by playing with their ratio in the mixed solution, which

allows a precise control of the composition of the multilayered film.

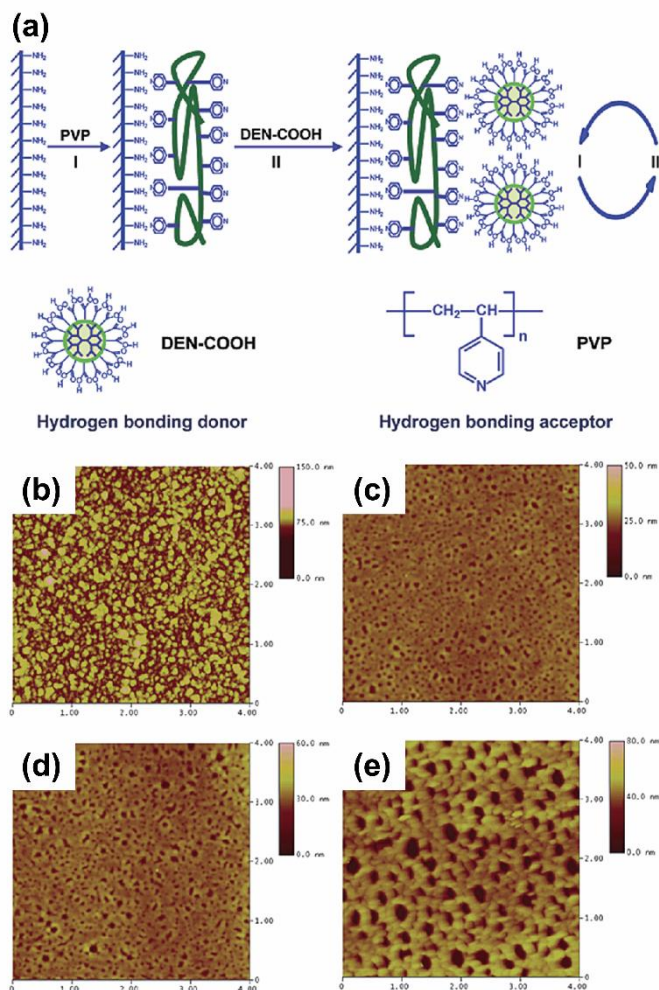


**Fig. 8** (a) Schematic drawing showing the growth of PVP/DEN-COOH multilayered films on a  $\text{NH}_2$ -modified quartz substrate based on hydrogen bonding: adsorption of (I) PVP and (II) DEN-COOH. AFM images of a  $(\text{PVP}/\text{DEN-COOH})_{14}$  multilayered film deposited onto a quartz substrate after immersion in a basic solution for (b) 10, (c) 30, (d) 60 and (e) 180 min. Adapted from ref. 130 with permission from the American Chemical Society.

### 2.2.3 Influence of solution pH

Weak poly(carboxylic acid)s, such as poly(methacrylic acid) (PMAA) and PAA, are often employed as hydrogen bonding donors to construct hydrogen bonding-based LbL films by combining them with hydrogen bonding acceptor polymers, such as PAMAM-COOH.<sup>137</sup> LbL films encompassing PMAA and PAMAM-COOH were successfully prepared by combining electrostatic interactions and hydrogen bonding, in acidic media ( $\text{pH} 4$ ).<sup>138</sup> Although the main interaction responsible for the successful deposition of these films at  $\text{pH} 4$  (Fig. 9a) is hydrogen bonding, the films decomposed in strongly acidic ( $\text{pH} 2$ ) (Fig. 9b) and neutral  $\text{pH}$  (Fig. 9a). The decomposition of LbL films at  $\text{pH} 2$  is unexpected because even at this  $\text{pH}$  the hydrogen bonding should be formed, which confirms that besides the hydrogen bonding, electrostatic interactions play a key role in the development of PMAA/PAMAM-COOH multilayered films. The tertiary amines in PAMAM have a  $\text{p}K_a$  of 6.3, and consequently at  $\text{pH} 4$ , they are positively charged, which aids PMAA in binding to PAMAM-COOH. In contrast, at  $\text{pH} 2$ , PMAA is completely protonated, so without

electrostatic affinity to the dendrimer. On the other hand, at pH 7, a large fraction of carboxylate groups in PMAA and PAMAM dendrimers are negatively charged and, thus, no complex formation has been observed. Therefore, PMAA/PAMAM-COOH films are stable only when hydrogen bonding and electrostatic interactions are simultaneously available. Thus, the pH-sensitive nature of LbL films based on hydrogen bonding is highly useful for the development of pH-triggered delivery systems.

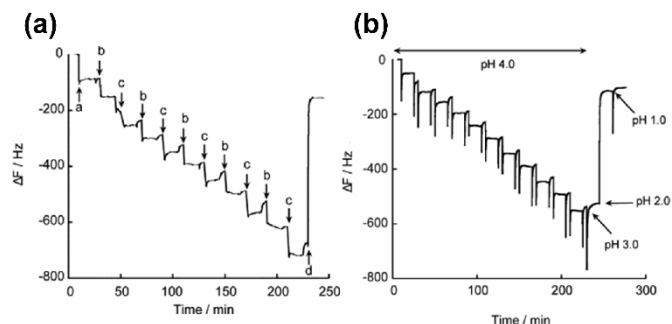


**Fig. 9** (a) QCM data for the creation of a (PMAA/PAMAM-COOH)<sub>5</sub> multilayered film at pH 4 and its decomposition at pH 7. The quartz resonator was exposed to (a) PEI, (b) PMAA, (c) PAMAM-COOH solutions and (d) 50 mM phosphate buffer, pH 7. (b) QCM response for the decomposition of a (PMAA/PAMAM-COOH)<sub>5</sub> multilayered film in strong acidic conditions. Adapted from ref. 138 with permission from the Elsevier.

In another interesting contribution, Park *et al.* reported the preparation of multilayered films enclosing block copolymer micelles derived from amphiphilic poly(2-ethyl-2-oxazoline)-block-poly( $\epsilon$ -caprolactone) (PEtOZ-PCL) and PAMAM-COOH at pH 3 via hydrogen bonding.<sup>139</sup> The PEtOZ outer shell of the micelle afforded the pH-responsive hydrogen bonding sites to the PAMAM-COOH. It was observed that, after the immersion in an aqueous solution at pH 3, the multilayered film showed densely packed micelles. On the other hand, the dipping of such films in an aqueous solution at pH  $\geq 5.6$  revealed that the multilayered film was removed in a reversible manner since the hydrogen bonding between the PEtOZ shell of the PEtOZ-PCL micelle and the PAMAM end groups was vanished. Moreover, PEtOZ-PCL micelle was loaded with a dye (disperse red 1), showcasing that most of the micelles were released from the multilayered film after 1 min of immersion in an aqueous solution at pH 5.6. Such pH-sensitive behavior turns the multilayered films into very appealing carrier vehicles to control the encapsulation and release of the drugs in different pH environments.

### 2.3 Covalent bonding

The use of covalent bonds to assemble LbL films provides a mean to enhance the stability and strength of the multilayered structure. Covalent bonding provides flexibility in the selection of molecules, where moderately charged or even uncharged molecules can be employed within the multilayered structure, allowing the development of multifunctional assemblies.<sup>83,140</sup> Although covalent-based multilayers are remarkably stable and have been investigated in a high number of applications, this approach requires chemical affinity between the molecules to be adsorbed, which limits their choice.<sup>141</sup> Moreover, if one envisions the preparation of stimuli-responsive and dynamic multilayers, the covalent-based systems are not generally appropriate due to their irreversibility.

The preparation of covalent-based polymeric assemblies was firstly proposed by Crooks and co-workers, who reported the LbL assembly

of multilayered thin films through the alternate deposition of poly(maleic anhydride)-*c*-poly(methyl vinyl ether) (Gantrez) and amine-, hydroxyl-terminated PAMAM or amine-terminated PPI dendrimers, resulting in a densely functionalized and organized film.<sup>142,143</sup> The current resulting from multilayered films encompassing hydroxyl-terminated PAMAM-coated electrode was larger when compared with the response of composite films comprising amine-terminated PAMAM and PPI dendrimers. Moreover, it was shown that films composed of amine-terminated dendrimers revealed a pH-dependent behavior as the result of the internal film morphology owing to the different linking chemistry and their amphoteric character once they simultaneously present amine and carboxylic groups, which were derived from the unreacted primary and tertiary amine groups of dendrimers, and amic acid groups resulting from Gantrez linking, respectively. Besides, the effect of the thermal treatment was also assessed, showcasing that the heating causes changes in the functional groups' composition, and decreases the film thickness. In the case of films comprising Gantrez and amine-terminated PAMAM, the heating led to a decrease in the amide band intensity and the emergence of two imide peaks at 1710 and 1722 cm. Similarly, films incorporating Gantrez and amine-terminated PPI showed the disappearance of the amide peaks and the appearance of two new bands typical of imides. In which concerns to the thermal treatment of the films developed with Gantrez and hydroxyl-terminated PAMAM, the authors denoted the formation of two imide bands, which increase in intensity with increasing the heating time. The authors hypothesized that the imide groups were formed between the amic acid groups derived from the reaction of Gantrez with NH<sub>2</sub>-modified surface and the amine end groups in the dendrimers. This methodology is a novel approach for the preparation of thin films, where the coupling of a reactive surface to a polyfunctional polymer leads to a covalently attached reactive brush, that in turn allows the preparation of a multilayered structure through the incorporation of a reactive dendrimer substrate. PAMAM or ferrocenyl-tethered dendrimers and an aldehyde-enzyme were also used for the fabrication of LbL films driven by covalent bonding.<sup>144</sup> In this regard, the hydroxyl groups in the surface of glucose oxidase (GOx) were oxidized, by periodate, into aldehyde groups and then reacted with the amine groups on an Au electrode surface through a Schiff base reaction. The remaining aldehyde groups of GOx reacted with amino groups on PAMAM dendrimers or ferrocenyl-tethered dendrimers (Fig. 10), resulting in a well-ordered and stable multilayered film on the Au electrode surface.

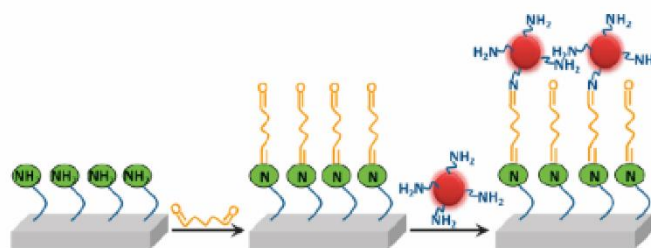


**Fig. 10** Illustrative scheme of the preparation of multilayered films based on the adsorption of an aldehyde-enzyme mediated Schiff base reaction onto a flat solid substrate. Reprinted from ref. 144 with permission from the American Chemical Society.

LbL films composed of PAMAM-COOH and nitro-containing diazoresin (NDR) were submitted to UV irradiation (Fig. 11a) for different times (Fig. 11b) in order to change the linkage between the multilayers from ionic to covalent, which improves considerably the

robustness and stability of the films.<sup>145,146</sup> It was shown by AFM measurements that the (PAMAM-COOH/NDR)<sub>4</sub> multilayered film was rather flat, with a mean roughness of only 1.4 nm, confirming the successful formation of a uniform multilayered film encompassing PAMAM-COOH and NDR. In contrast, prior to UV irradiation, the molecules were compressed in the films due to the strong ionic interactions between PAMAM-COOH and NDR, and the soft nature of dendrimer architecture. Similarly, multilayered films encompassing Ag-dendrimer nanoclusters and DR were developed (Fig. 11c), denoting better electric conductivity when compared to the LbL films without Ag nanoclusters.<sup>147</sup> Besides, AFM measurements disclosed that, prior to the UV irradiation, the LbL films were destroyed after 1 h of etching (Fig. 11d) whereas the irradiated film showed good resistance to the same process (Fig. 11e).

In 2001, Sharpless and co-workers introduced the concept of click chemistry in an effort to focus on the easy production of properties rather than challenging structures.<sup>148</sup> The idea was to confine the whole range of chemical transformations to a set of reactions with a high thermodynamic driving force, allowing the efficient and easy transformation of “spring-loaded” starting materials into new structures with useful properties.<sup>149</sup> The impact of click chemistry has been significant in polymer synthesis, an area where reaction efficiency and product purity are significantly challenged.<sup>150</sup> Among the click reactions, the copper(I)-catalyzed azide-alkyne cycloaddition (CuAAC) has emerged as the archetypal example owing to its high orthogonality, and reactivity and regioselectivity, leading exclusively to 1,4-disubstituted 1,2,3-triazoles.<sup>151,152</sup> Li *et al.* reported the preparation of hybrid multilayered films encompassing an azide-functionalized poly(4-vinyl benzaldehyde) (P(VBA-AA)) and alkyne-functionalized polyphenylene dendrimer-capped AuNPs (G2SH-AuNPs).<sup>153</sup> It was found that the deposition process is linearly dependent on the number of bilayers, which was confirmed by the absorption peak at 260 nm, corresponding to the complex formation between Au and the carboxyl group. The multilayered film can be potentially applied as vapor-sorption and electrical chemiresistors for the 3D structure of polyphenylene dendrimers.

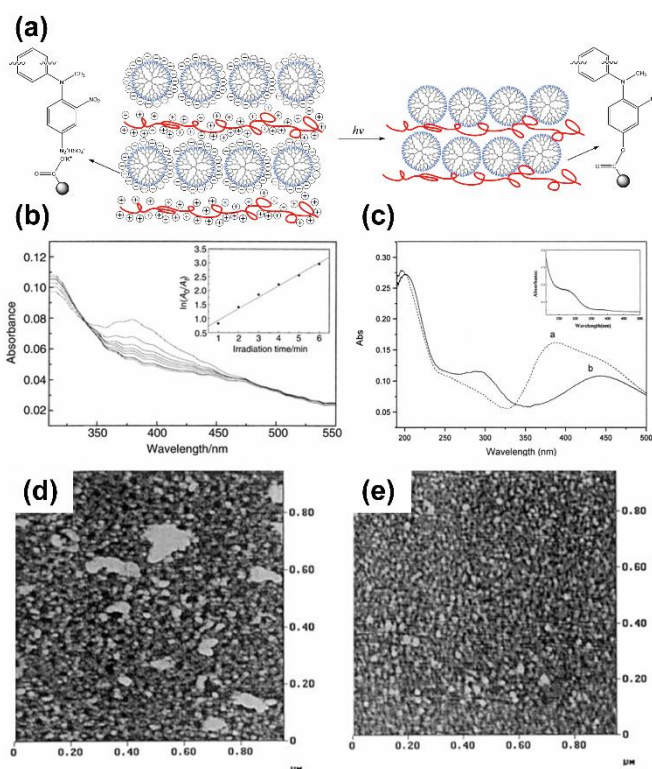


**Fig. 11** (a) Development of LbL films composed of PAMAM-COOH and NDR, and conversion of the interlayer linkage bonds from ionic to covalent upon UV irradiation. (b) UV-Vis absorption spectra of a (PAMAM-COOH/NDR)<sub>12</sub> multilayered film irradiated during (top to bottom) 1, 2, 3, 4, 5, 6, 10, 20 and 30 min. The inset figure shows the photodecomposition of the film, where  $A_0$  and  $A_1$  represent the absorbance of the film before and after UV irradiation at different times, respectively. Adapted from ref. 146 with permission from the Royal Society of Chemistry. (c) UV-Vis absorption spectra of a Ag-PAMAM-COOH/DR multilayered film (a) before and (b) after UV irradiation. The inset shows the UV-Vis absorption spectra of the multilayered film without Ag nanoclusters. AFM images of a Ag-PAMAM-COOH/DR multilayered film (d) before and (e) after UV irradiation. Adapted from ref. 147 with permission from the Wiley-VCH Verlag GmbH & Co.

These results emphasize the potential of the covalent bonding-based LbL assembly via CuAAC for preparing uniform polymer/NP hybrid thin films with controlled thickness. Moreover, this is an attractive strategy to develop multilayered assemblies with noncharged polymers and NPs.

Furthermore, the covalent bonding driven LbL assembly affords cell surface engineering. Gattás-Asfura *et al.* reported the efficient preparation of conformal and covalently stabilized nanocoatings on pancreatic islets by functionalizing them with oppositely charged hyperbranched alginate (ALG) biopolymer and PAMAM dendrimer enclosing complementary Staudinger ligation groups (another click reaction), respectively azide groups and methyl-2-(diphenylphosphino)terephthalate (Fig. 12).<sup>154,155</sup> The functionalization of the PAMAM dendrimer with triethoxysilane reduced the dendrimer charge density and triggered its self-assembly capability during the layer formation, further enabling the stable covalent-based LbL nanoencapsulated islets to maintain high cell viability and functionality, lack foreign body responses, and enable stable normoglycemia after implantation in diabetic mice. Such conformal and stable covalent-based LbL nanocoatings have

the ability to bioorthogonally tether supplemental agents to the surface, including proteins, via Staudinger ligation chemistry offering the possibility to modulate the implant microenvironment and be used in the immunoprotection of islets for the treatment of diabetes.

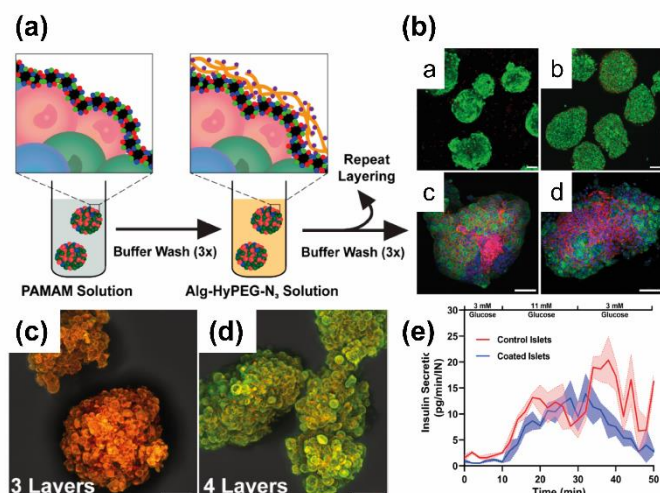


**Fig. 12** (a) Schematic representation of the LbL assembly process comprising alternating layers of functionalized PAMAM and ALG assembled on islets via covalent bonding. (b) Confocal laser scanning microscopy (CLSM) images of live (green) and dead (red) staining on (a) uncoated (control) and (b) coated islets. Z-stack projection confocal images of layer formation on pancreatic islets, building from (c) three and (d) four alternating layers of functionalized PAMAM and ALG. Whole mount immunohistochemistry imaging of insulin (green), f-actin (red), and nuclei (blue) (c) uncoated control and (d) four-layer coated islets. Scale bar = 50  $\mu\text{m}$ . (e) Dynamic glucose stimulated insulin release for uncoated control (red) and four-layer coated (blue) islets. Adapted from ref. 155 with permission from the American Chemical Society.

In conclusion, covalent-based LbL assembly is a powerful and efficient approach to construct highly stable, well-ordered and robust ultrathin multilayered films and nanocomposites with structural precision and flexible design, thus demonstrating its potential to tailor the film properties by the careful selection of its components.

## 2.4 Coordination chemistry interactions

Coordination chemistry are strong intermolecular interactions established between a wide selection of organic ligands and transition metal ions, enabling the design and preparation of novel, well-ordered, and highly oriented LbL assemblies. This approach allows controlling the surface structure at the molecular level via the synthesis of deliberately designed ligands.<sup>83,156</sup>

Despite the great interest in combining dendritic growth on surfaces with coordination chemistry, there are only a few studies in the literature that report the formation of multilayered thin films by exploiting the coordination of metal ions to dendrimers. Watanabe and Regen developed LbL films consisting of PAMAM dendrimers and  $\text{Pt}^{2+}$  via LbL assembly driven by coordination chemistry (Fig. 13).<sup>65</sup> They hypothesized that by resorting to appropriately-size dendrimers, attractive gels could be developed and applied to fabricate catalysts or as a basis for optical filters and devices. Blasini and co-workers prepared multilayered films encompassing terpyridyl-pendant PAMAM dendrimers and  $\text{Co}^{2+}$  onto a silicon oxide ( $\text{SiO}_2$ ) surface and demonstrated that the coordination between the dendrimers and  $\text{Co}^{2+}$  ions is strong, conducting to a compression or deformation of the film with decreased height of the dendrimer.<sup>157</sup> Furthermore, metal ions have been also successfully employed to

fabricate multilayered films encompassing peptide dendrimers on Au surfaces functionalized with 11-mercaptopundecanoic acid. In this regard, Appoh and Kraatz observed that metal ions prefer to coordinate to the carboxylic acid residues when compared to the peptide backbone.<sup>156</sup> The good compatibility of those films could arouse much interest for the design of NPs for nanomedicine.

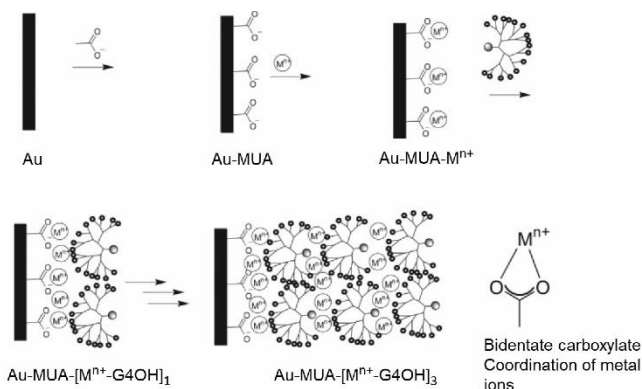


**Fig. 13** Schematic representation of the LbL assembly process for the alternate adsorption of dendrimers and metal ions onto a modified Au substrate via coordination chemistry. Reprinted from ref. 156 with permission from the Wiley-VCH Verlag GmbH & Co.

## 2.5 Host-guest interactions

LbL films can also be created using highly selective and specific host-guest interactions, by exploring the strong interactions between host (e.g., cyclodextrins, calixarenes, crown ethers, porphyrins) and guest (e.g., ferrocene, adamantane, azobenzene) molecules.<sup>83,158</sup> Huskens and co-workers reported the build-up of organic/inorganic hybrid multilayered films with controlled thickness based on selective host-guest interactions between host cyclodextrins-modified AuNPs (CD-AuNPs) and guest adamantyl-functionalized PPI dendrimers (Fig. 14a).<sup>159</sup> CD-AuNPs and PAMAM or PPI dendrimers decorated with ferrocenes can also be used to create thin films that take advantage of the superior features of dendrimers and the function of metals (Fig. 14b).<sup>160</sup> In both cases, the multilayers were deposited onto CD self-assembled monolayers (SAMs) on Au or  $\text{SiO}_2$  surfaces and, the multivalent host-guest interactions between the dendrimer end groups and the CD-AuNPs, led to the formation of well-defined and stable surface patterns by "supramolecular microcontact printing" (Fig. 14c,d).

Furthermore, Huskens and co-workers developed patterned LbL assemblies on the CD SAMs by nanotransfer printing (nTP) and nanoimprint lithography (NIL) once the LbL assembly was prevented on chemically patterned SAMs by microcontact printing or NIL owing to the low specificity of the adsorption of the dendrimer.<sup>161</sup> The differences in thickness of the LbL films produced by nTP or NIL approaches were attributed to rinsing or remove procedures, as well as to the differences in wetting. Overall, the preparation of organic/inorganic hybrid multilayered films based on multivalent host-guest interactions between host-modified AuNPs and dendritic guest molecules was successfully reported. Furthermore, the z control when combined with top-down surface patterning methods, such as soft lithography, for x, y control, allows the creation of 3D supramolecular multilayered assemblies. As such, these films are very appealing in the fabrication of electronic and optical devices, in which the structural design at the nanometer scale level leads to superior performance and new functionalities.

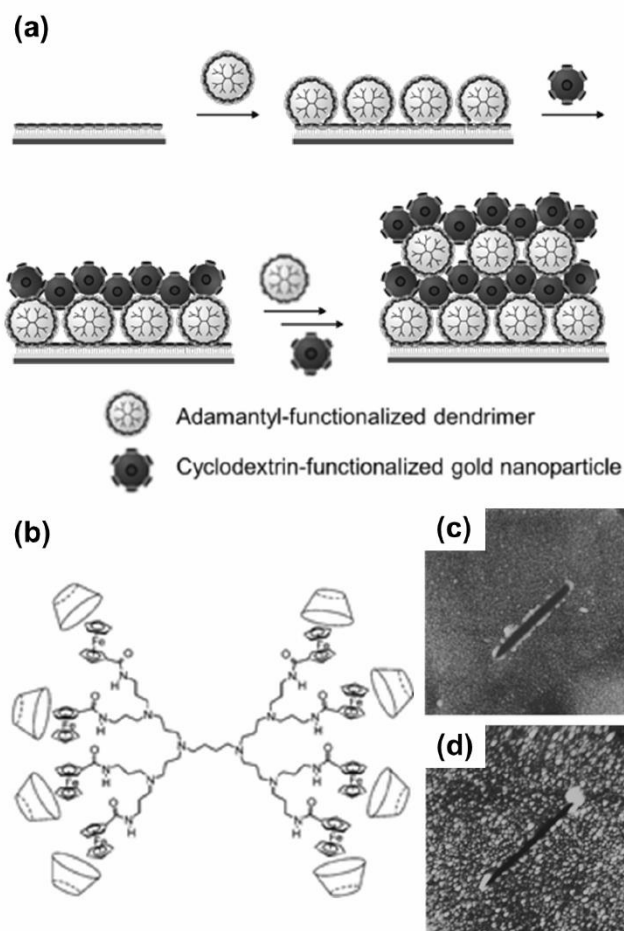


**Fig. 14** (a) Schematic illustration of the LbL assembly process comprising alternating layers of adamantyl-functionalized PPI dendrimer and CD-AuNPs onto CD SAMs via host-guest interactions. Adapted from ref. 159 with permission from the American Chemical Society. (b) G2 PPI dendrimer with ferrocene end groups complexed with CD. Adapted from ref. 160 with permission from the Royal Society of Chemistry. AFM images of (c) one bilayer and (d) four bilayers composed of adamantyl-functionalized PPI dendrimer and CD-AuNPs deposited onto a CD SAM. The image size in (c) is 20 nm x 1.2  $\mu$ m and in (d) is 10 nm x 1.2  $\mu$ m. Adapted from ref. 159 with permission from the American Chemical Society.

## 2.6 Biologically specific interactions

Biologically specific interactions can also be used to create multilayered films. These intermolecular interactions encompass a broad range of interactions, such as electrostatic and hydrophobic interactions, and hydrogen bonding, enabling high specificity and functionality to the target molecules.<sup>83</sup> Biological specific interactions include avidin-biotin,<sup>162</sup> antibody-antigen,<sup>163</sup> lectin-carbohydrate interactions,<sup>164</sup> and DNA hybridization.<sup>165</sup>

### 2.6.1 Avidin-biotin interactions to build-up multilayered systems

LbL films prepared by the alternate deposition of fluorescein isothiocyanate (FITC)-avidin and biotin-labeled PAMAM dendrimers have been reported by Anzai *et al.* who demonstrated that one monolayer of avidin (tetrameric protein) is adsorbed per each PAMAM layer (Fig. 15a).<sup>166</sup> In contrast, multilayered films developed with linear and branched polymeric chains, such as PAA and PEI,

respectively, showed that for each layer of PAA (Fig. 15b) or PEI (Fig. 15c), multilayers of avidin are deposited. These results can be explained by the globular molecular geometry exhibited by PAMAM when compared with the branched structure denoted by PEI. Moreover, it was found that the films did not form when they were assembled with biotin-free polymers, thus corroborating that the binding between avidin and biotin is key for the formation of the multilayered films.

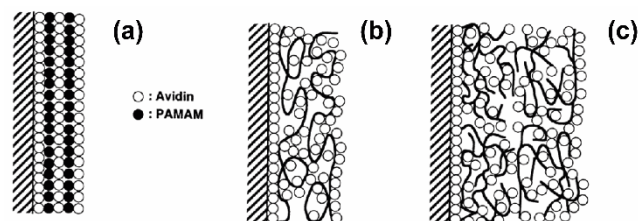


**Fig. 15** Possible structure of multilayered films composed of (a) FITC-avidin/biotin-PAMAM, (b) FITC-avidin/biotin-PAA and (c) FITC-avidin/biotin-PEI. Reprinted from ref. 166 with permission from the American Chemical Society.

The authors also studied the effect of the concentration of the materials in the preparation of FITC-avidin/biotin-poly(amine)s films. It was seen that, in the case of the FITC-avidin/biotin-PEI films, the PEI can accommodate FITC-avidin molecules either inside or on the surface of the biotin-PEI layer, providing a disheveled multilayered surface, where the loading of FITC-avidin depends on its concentration in the solution. The deposition with a solution of 100  $\mu$ g/mL led to the formation of 5-6 layers of FITC-avidin on the slide upon each deposition whereas a solution of 10  $\mu$ g/mL enabled nearly monomolecular deposition of FITC-avidin. Multilayered films comprising biotin-PAA showed a similar behavior but with a lower loading of FITC-avidin when compared to the FITC-avidin/biotin-PEI films. Interestingly, the authors observed that the loading of FITC-avidin in the FITC-avidin/biotin-PAMAM films was slightly dependent on the concentration of FITC-avidin in solution, which led to a nearly monomolecular layer of FITC-avidin absorbed upon each deposition step, confirming that the driving force is the avidin/biotin complexation. The different behavior was attributed to the molecular architecture of the polymers. Besides, the adsorption of FITC-avidin is faster in biotin-PAMAM than in biotin-PEI films. In fact, just 10 min are needed for the complete adsorption of FITC-avidin onto a biotin-PAMAM layer whereas 60 min are needed for the adsorption onto biotin-PEI. The faster adsorption of avidin onto biotin-PAMAM is due to the globular architecture of PAMAM, providing increasing accessibility sites for the adsorption of avidin and formation of avidin-biotin complexes. Moreover, PEI has a higher positive surface charge density than PAMAM and once the FITC-avidin is also positively charged under the experimental conditions, the electrostatic repulsion between biotin-PEI and FITC-avidin led to a lower adsorption rate than in the case of biotin-PAMAM films. As such, a judicious choice of the polymeric materials allows the regulation of the loading of the biomaterials in multilayered films driven by biological specific interactions. Moreover, the functionality of those films can be improved using modified avidin residues, namely avidin-enzyme and avidin-antibody conjugates or poly(amine)s containing biotin and other functional groups in their side chains which allow the development of functional films with a controlled density of functional groups.

## 2.6.2 DNA hybridization to assemble and growth multilayered assemblies

DNA has aroused much interest due to its high biocompatibility and biodegradability and, as such, many systems enclosing DNA have been developed for addressing applications in the biomedical and biological fields, including diagnostics, therapeutics and biosensing. Although the preparation of LbL assemblies incorporating DNA have been predominantly accomplished via electrostatic interactions, owing to its negative charge, DNA can also be incorporated in LbL systems by resorting to biologically specific interactions, including DNA hybridization that allow the assembly of species with the same charge. In this regard, Feng *et al.* reported the DNA hybridization driven encapsulation of a dye molecule (Cy5) into multilayered microcapsules with shells composed of alternating layers of phosphorous dendrimers and PSS.<sup>167,168</sup> The hybridized double stranded DNA can be further dehybridized by applying an external stimulus, such as SDS or sodium phosphate (NaHPO<sub>4</sub>) which would allow to control the release of Cy5. Therefore, this approach would be useful for the encapsulation of low molecular weight molecules that are difficult to encapsulate by other methods due to their easy diffusion through the capsule's shells. Moreover, the encapsulation of molecules into well-defined dendrimer-based capsules is possible without adjusting parameters, such as shell permeability by solvents, chemical oxidation, ionic strength or pH, which considerably improve the probability of destroying the shell or denature encapsulated biomolecules.

The construction of supramolecular multilayered assemblies by resorting to biologically specific interactions enables the incorporation of a wide array of materials, resulting in films with enhanced stability and orientation. These films denote great potential for being applied in the fabrication of biosensors, as well as in diagnostics and molecular biology.

## 3. Bioapplications of dendrimer-containing LbL assemblies

The supramolecular dendrimer-containing LbL assemblies offer an enhanced control over the multilayer composition, structure, properties and functions in comparison to the conventional linear polymer-based LbL systems due to the well-defined hyperbranched and globular architecture, high surface area, and tunable nanosize, molecular weight, chemical composition and surface functionality of dendrimers. As such, dendritic-based LbL architectures have aroused much interest in a wide variety of biological and biomedical applications, including in biosensing, bioimaging, drug/therapeutics delivery, and gene therapy.

### 3.1 Biosensing

Monitoring biological and biochemical processes is essential when aiming for biological and biomedical applications. In fact, the development of highly sensitive, specific, and cost-effective biosensors contributes to the creation of an accurate diagnosis and personalized medicine. Nowadays, sensors allow the detection of not only the more traditional class of biomarkers (e.g., nucleic acids, proteins) but also metabolites and pathogens, thus increasing the

range of available techniques for an individual's diagnosis.<sup>169</sup> Biosensors are usually developed using electrodes or transducers coupled with biorecognition elements, such as enzymes, antibodies, DNA or aptamers. Moreover, the immobilization of proteins on the surface of transducers without losing their biological activity is a key issue while designing biosensors. As such, LbL films enclosing proteins have been widely studied to improve the recognition and transducer processes in biosensors.<sup>170,171</sup>

Dendrimers have been used in the preparation of biosensors by three main strategies: 1) producing surface monolayers as scaffolds for the immobilization of proteins, 2) creating LbL films comprising dendrimers and proteins and, 3) encapsulating or covalent binding metal NPs and electron transfer mediators. In fact, dendrimers have been used to modify the surface of electrodes with monolayer films, on which proteins are further immobilized. For instance, biosensors encompassing monolayers of PAMAM dendrimers on the surface of Au or Ag substrates further modified with proteins or single-stranded DNA have been reported.<sup>172,173</sup>

Furthermore, multilayered films composed of dendrimers and enzymes have also been proposed for biosensing. In this regard, multilayered films encompassing PAMAM and GOx were developed via electrostatic interactions and it was observed that, after the assembly of two bilayers, the further deposition of GOx layers did not improve the response of the glucose biosensors (Fig. 16a).<sup>174</sup> Similarly, LbL films comprising PAMAM layers covalently coupled to GOx via a Schiff base linkage on the surface of Au electrodes showed that the response of glucose biosensors increased while increasing the number of GOx/PAMAM bilayers up to 5 (Fig. 16b), confirming that the catalytic activity was maintained in the LbL film.<sup>175</sup> These results indicated that the design of glucose biosensors through covalent bonding driven GOx/PAMAM LbL films is stronger than similar films assembled by electrostatic interactions.

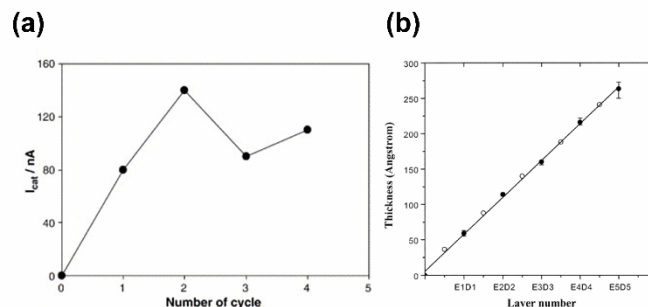


**Fig. 16** (a) Catalytic current response as a function of the cycle number in multilayered films comprising PAMAM and GOx on Au surfaces via electrostatic interactions. Adapted from ref. 174 with permission from the Elsevier. (b) Evolution of the ellipsometric thickness of the GOx/PAMAM multilayers assembled on Au surfaces via covalent bonding as a function of the number of layers. Open circles show the thickness of GOx-terminated multilayers. Reprinted from ref. 175 with permission from the American Chemical Society.

Heme proteins, including hemoglobin (Hb), myoglobin (Mb), and catalase (Cat) have been also used to create electrostatically-driven multilayered films with PAMAM dendrimers on an array of solid surfaces.<sup>176</sup> In this regard, PAMAM/protein multilayered films were developed and exploited as enhanced systems to catalyze substrates with biological and/or environmental significance. PAMAM/Hb and PAMAM/Mb multilayered films showed better stability than PAMAM/Cat films, without significant decrease of the peak current. PAMAM/Cat multilayered films disclosed a decreased of *c.a.* 20%

compared to the initial peak current value. The decrease in the reduction overpotential together with the good stability and sensitivity of the LbL films suggest their usefulness as electrochemical biosensors or bioreactors without the need of mediators, in which the electrochemical and electrocatalytic activity can be regulated by adjusting the thickness of the films.

Metal NPs-encapsulating dendrimers have been also successfully and intensively employed to create sensitive enzyme-containing LbL films for biosensing. For example, PPI-Au nanoclusters were successfully assembled with Mb into PPI-Au/Mb LbL films on the surface of graphite electrodes and showed better electrochemical properties and catalytic activity than similar PPI/Mb and PAMAM/Mb LbL films due to the good conductivity assigned to the AuNPs, which play a key role in the electron transfer of Mb in the LbL films.<sup>177</sup> Almost at the same time, Li and co-workers developed a glucose biosensor through the LbL alternating deposition of platinum NPs (PtNPs)-encapsulating PAMAM dendrimer and oppositely charged GOx on Pt electrodes and showed that the response of the biosensor was significantly enhanced in the presence of the PtNPs, indicating that these procedures can be useful for creating efficient microelectrodes.<sup>178</sup> Moreover, an electroanalytical glucose biosensor was also developed through a polypyrrole (PPy) film doped with PAMAM dendrimers-encapsulating PtNPs (Pt-PAMAM-PPy) and GOx, aiming for triggering the electrocatalytic oxidation of glucose.<sup>179</sup> The resulting film showed good stability with improved electrocatalytic activity, thus suggesting that glucose can easily permeate porous composite films.

Besides, LbL films composed of dendrimers have been also applied as gate materials for field effect transistor biosensors. Siqueira *et al.* reported the preparation of multilayered films encompassing PAMAM and carboxylate single-walled carbon nanotubes (SWNT), further modified by the immobilization of penicillinase on the top of the film surface for producing penicillin biosensors (Fig. 17a).<sup>170,180</sup> The LbL films showed to be highly porous due to the interpenetration of SWNTs into the dendrimer layers. Moreover, a good sensitivity to pH (Fig. 17b,c) and biosensing ability towards penicillin was shown by an electrolyte-insulator-semiconductor (EIS) structure modified with carbon nanotubes (EIS-NT)-penicillinase biosensor.

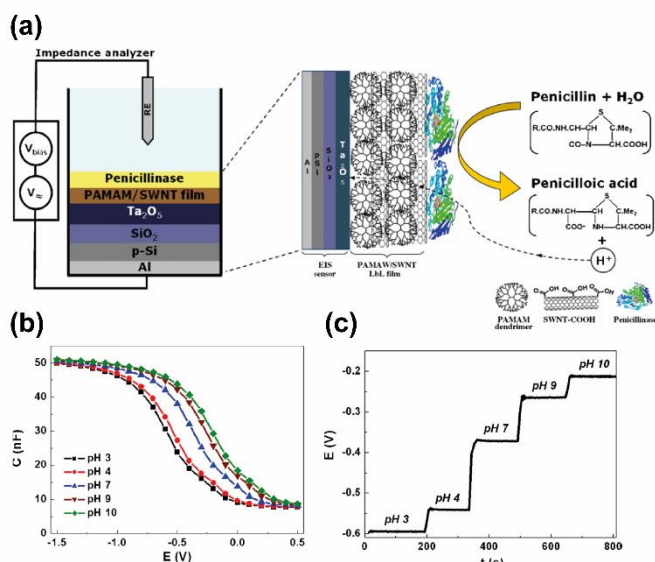


**Fig. 17** (a) Oversimplified representation of the structure, operation principle and chemical reaction of the penicillin biosensor based on an EIS structure functionalized with multilayered films encompassing PAMAM and SWNT. (b) Capacitance-voltage curves and (c) constant-capacitance response at

different pH values for an EIS-NT sensor. Adapted from ref. 180 with permission from the Elsevier.

As such, there is no doubt about the potential of dendrimer-derived LbL assemblies for biosensing. Despite the different mechanisms involved in the development of biosensor-based LbL films, those enclosing metal NPs-encapsulating dendrimers showed to be promising owing to their better electrocatalytic properties and stability, thus suggesting their potential use as efficient electrodes. Therefore, a careful selection of the methodology and building blocks to be used enables the design of multilayered films able to be applied in various analytical applications in the biotechnology field.

Furthermore, an important tool in biomedicine is bioimaging. The first *in vivo* applications of dendrimers were as macromolecular magnetic resonance imaging (MRI) contrast agents.<sup>5,181</sup> In this regard, the incorporation of dendrimers in multilayered films has aroused much attention in biomedicine, in particular, in the field of diagnostics. For instance, iron oxide ( $\text{Fe}_3\text{O}_4$ ) NPs functionalized with LbL films have been prepared for targeting and imaging of cancer cells. For this purpose,  $\text{Fe}_3\text{O}_4$  nanoparticles were coated with PSS and folic acid (FA)- and FITC-tagged PAMAM dendrimer layers via electrostatic interactions, followed by an acetylation reaction to neutralize the still present amine groups on the surface of the dendrimers.<sup>182</sup> The authors showed that  $\text{Fe}_3\text{O}_4/\text{PSS}/\text{G5-NHAc-FITC-FA}$  NPs can target FA receptors that are overexpressed in the surface of cancer cells (Fig. 18).

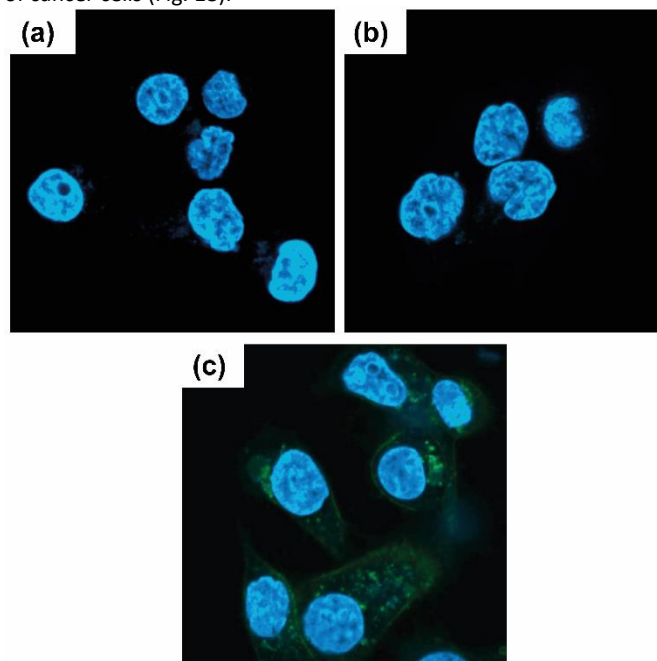


**Fig. 18** CLSM images of KB-KFAR cells treated with (a) phosphate buffered saline, (b)  $\text{Fe}_3\text{O}_4/\text{PSS}/\text{G5-NHAc-FITC}$  NPs and (c)  $\text{Fe}_3\text{O}_4/\text{PSS}/\text{G5-NHAc-FITC-FA}$  NPs. The nucleus of cells was stained in blue with Hoescht 33342. The green color was originated from the FITC-conjugated dendrimers. Reprinted from ref. 182 with permission from the Wiley-VCH Verlag GmbH & Co.

As such, this study describes a striking methodology for creating various nanosized imaging agents for biosensing and therapeutic applications, since these type of materials have ability to be specifically located in tumors via enhanced permeation and retention effect that in turn allow an enhanced imaging sensitivity and specificity.<sup>183,184</sup>

### 3.2 Drug/therapeutics delivery

The design of smart modular platforms that could promote the efficient encapsulation, protection, transport, and orchestrated intracellularly controlled and sustained release of bioactive agents would represent a hallmark in advanced therapeutic systems. In particular, the unique features of dendrimers,<sup>185</sup> and the high versatility of LbL assemblies<sup>104</sup> have contributed to the development of novel surface-mediated drug delivery systems. Dendrimer-containing multilayered films provide enhanced binding sites to drugs via the internal cavities of dendrimers and their terminal functional groups, as well as those of the multilayered film. Moreover, their integration with stimulus-sensitive materials has gathered considerable attention in the development of controlled drug delivery systems. To achieve this goal, LbL films sensitive to pH,<sup>186,187</sup> salts,<sup>188</sup> temperature,<sup>189,190</sup> sugars,<sup>191,192</sup> and electrical signals<sup>193–195</sup> have been widely exploited. For instance, Sato and Anzai created sugar-sensitive multilayered films enclosing poly(vinyl alcohol) (PVA) and phenylboronic acid-bearing PAMAM dendrimer (PBA-PAMAM) via boronate ester chemistry between the boronic acid moiety in PBA-PAMAM and the 1,3-diol units in PVA.<sup>196</sup> These LbL films were used as a sacrificial layer for preparing free-standing multilayered membranes composed of PSS and poly(allylamine hydrochloride) (PAH) (Fig. 19). The authors demonstrated that external stimulus, including pH changes, salts and sugar induced the release of the free-standing PSS/PAH multilayered membranes from PVA/PBA-PAMAM/PSS/PAH films showcasing the highest release rate in the presence of solutions of higher sorbitol concentrations (5–15 mM), pH 9 and lower NaCl concentrations (150 mM). As such, this is certainly a useful approach for developing free-standing multilayered membranes enclosing pH-sensitive materials, including proteins.

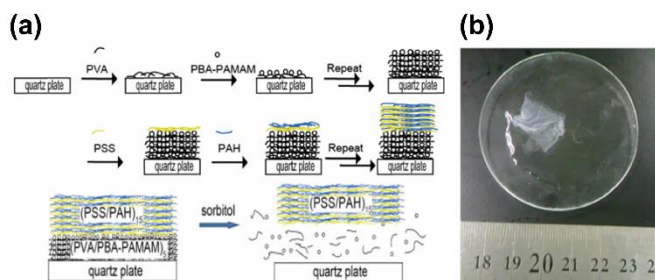


**Fig. 19** (a) Schematic drawing showing the development of (PVA/PBA-PAMAM)<sub>5</sub>/(PSS/PAH)<sub>15</sub> multilayered films (top) and sorbitol-induced release of the PSS/PAH film from the substrate (bottom). (b) Photograph of a released (PSS/PAH)<sub>15</sub> film. Adapted from ref. 196 with permission from the Elsevier.

Similar multilayered films, responsive to pH and sugar, have been reported. Those include PVA/4-PBA-PAMAM multilayered assemblies, which decompose in response to glucose or fructose at pH 7.4 and 9,<sup>197</sup> and alginate acid/PBA-PAMAM multilayered films, which disassemble when exposed to 5–30 mM fructose at pH 7.5.<sup>121</sup> Moreover, multilayered films encompassing GOx and PBA-PAMAM were found to be stable in pH 8.5, while decomposing in neutral and acidic media due to the cleavage of the boronate ester bond.<sup>198</sup> Suwa *et al.* reported that such films also decomposed in the presence of

glucose owing to the oxidative scission of the carbon-boron bond in the PBA residues of PBA-PAMAM by enzymatic production of hydrogen peroxide (H<sub>2</sub>O<sub>2</sub>). Anzai and co-workers developed later PBA-PAMAM/PVA multilayered films showcasing their stability at pH 9 and decomposition after the addition of H<sub>2</sub>O<sub>2</sub> (Fig. 20a).<sup>199</sup> In fact, the exposure of the films to 0.5 and 1 mM H<sub>2</sub>O<sub>2</sub> during 30 min triggered the release of 75% and 90% of the PBA-PAMAM from the (PBA-PAMAM/PVA)<sub>10</sub> films (Fig. 20b). Thus, PBA-PAMAM/PVA films containing GOx enzymatically produced H<sub>2</sub>O<sub>2</sub> after being exposed to 1 mM glucose aqueous solution at pH 7.4 (Fig. 20c). Therefore, those multilayered assemblies show great promise for being used in drug/therapeutics delivery in response to reactive oxygen species and oxidative stress.

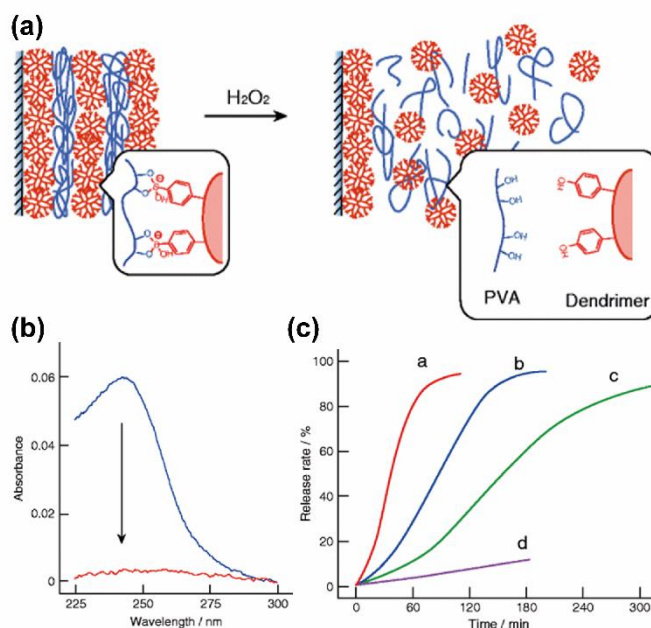


**Fig. 20** (a) Schematic illustration of the H<sub>2</sub>O<sub>2</sub>-induced release of PBA-PAMAM from PBA-PAMAM/PVA multilayered films. (b) UV-Vis absorption spectra of a (PBA-PAMAM/PVA)<sub>10</sub> multilayered film before (blue) and after (red) exposure to 1 mM H<sub>2</sub>O<sub>2</sub> in pH 9 for 30 min. (c) PBA-PAMAM release profile of (a) (PAH/GOx)<sub>3</sub>(PBA-PAMAM/PVA)<sub>10</sub>, (b) (PAH/GOx)<sub>2</sub>(PBA-PAMAM/PVA)<sub>10</sub>, (c) (PAH/GOx)<sub>1</sub>(PBA-PAMAM/PVA)<sub>10</sub> and (d) (PBA-PAMAM/PVA)<sub>10</sub> multilayered films in the presence of an 1 mM glucose aqueous solution. Adapted from ref. 199 with permission from the Springer Nature.

As aforementioned, hydrogen-bonded driven LbL films are usually pH-sensitive and decompose in strongly acidic and neutral pH. In this regard, PAMAM-COOH/PMAA films demonstrated to be sensitive to pH changes and decomposed upon exposition to buffer solutions at pH 2 and 7.<sup>138</sup> As such, these films have been used to load model dyes, such as Rose Bengal and sulfonated tetraphenylporphyrin, where the release is precisely controlled by pH changes. Besides, the construction of electrostatic-driven multilayered films composed of a negatively charged carboxylated Fréchet-type poly(aryl ether) dendronized polymer (denpol) loaded with water-insoluble pyrene dye and oppositely charged PDPA has been reported (Fig. 21a). It was shown that the release of pyrene from the multilayered films can be tuned by adjusting the ionic strength of the immersing solutions (Fig. 21b).<sup>200</sup> Moreover, it was shown that the pH of the polyelectrolyte solution influences the surface morphology and roughness of the dendrimer layer in the resulting films (Fig. 21c,d). Interestingly, the

authors found that the amount of pyrene released from the multilayered films can be reloaded by dipping the pyrene-released film into a saturated pyrene aqueous solution, disclosing the potential of the multilayered films for on-demand encapsulation and targeted release.

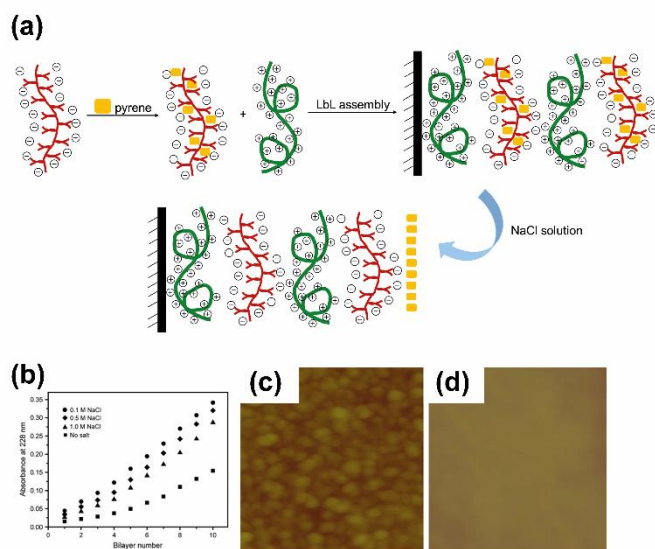


**Fig. 21** (a) Schematic illustration of the build-up of electrostatic-driven multilayered films comprising pyrene-loaded dendronized polymer and PDDA multilayers. (b) Effect of the ionic strength on the pyrene release kinetics from (PDDA/denpol)<sub>10</sub> multilayered films. AFM images of the outmost denpol layer in (PDDA/denpol)<sub>10</sub> LbL films with PDDA and denpol at (c) pH 6 and (d) pH 8. The scale bar is 500 nm x 500 nm. b-d: Adapted from ref. 200 with permission from the Elsevier.

The development of assembling methodologies for simultaneously enabling the covalent crosslinking of the multilayers and embedding drug reservoirs for retarded drug release has raised much interest in the biomedical field. In this regard, Schi and co-workers have developed a strategy for combining covalent interlayer linkages and drug reservoirs with a model drug.<sup>201</sup> For this purpose, LbL films composed of PAMAM-COOH dendrimers, serving as the drug reservoir, and PAH (Fig. 22a) were prepared. As expected, the immersion of the film in a sodium hydroxide (NaOH) aqueous solution at pH 12 for 30 min led to the almost complete disassembly of the PAMAM/PAH films (Fig. 22b) via deprotonation of the ammonium groups at PAH and fading of the attractive electrostatic attraction with the carboxyl groups in PAMAM. To improve the stability of the multilayers, a small bifunctional photoactive molecule, namely 4,4'-diazostilbene-2,2'-disulfonic acid disodium salt (DAS) was post-infiltrated in acidic conditions between the multilayers. This increased the protonation of PAH, thus contributing for improving the adsorption of DAS. The authors also observed that the infiltration process preserves the surface morphology of the layers, once that either before (Fig. 22c-a) or after DAS infiltration (Fig. 22c-b), as well as after UV irradiation (Fig. 22c-c), the substrate presented similar surface morphology and roughness. The obtained crosslinked PAH/PAMAM multilayers showed good stability and were organized in a rigid and compact structure, being able to retard the load and release of the model drug from the multilayers. The release profiles of small hydrophobic drug molecules, modeled by acridine orange (AO), through crosslinked and non-crosslinked multilayered films differed significantly, revealing similar trends to their absorption profiles. As such, the non-crosslinked loaded

multilayered films released around 98% of the AO during the first 5 min (Fig. 22d-a) whereas the crosslinked ones retarded the release of AO (Fig. 22d-b), with approximately 95% of the AO being released during the first 30 min. The crosslinking of PAH/PAMAM LbL films retained AO molecules for a much longer time than non-crosslinked ones due to the rigid globular shape of dendrimers, which imposes a powerful physical barrier for diffusion of AO both in-and-out of the film. Moreover, the crosslinked multilayered films showed the ability to withstand rising with ethanol, the most often used sterilization procedure, thus holding great promise for being used in a variety of biomedical scenarios.

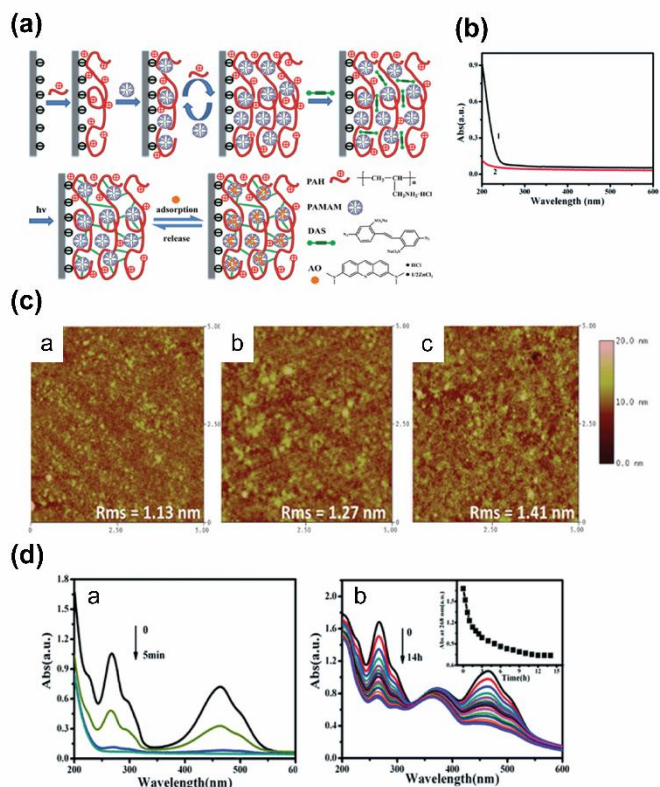


**Fig. 22** (a) Schematic representation of the preparation of PAH/PAMAM multilayered films and their stabilization with DAS, followed by adsorption of the hydrophobic molecules. (b) UV-Vis absorption spectra of (PAH/PAMAM)<sub>7.5</sub> multilayered films before (black) and after (red) immersion in NaOH aqueous solution at pH 12 on a modified quartz substrate. (c) AFM images of a (PAH/PAMAM)<sub>7.5</sub> multilayered film (a) before and (b) after DAS infiltration and (c) after UV irradiation. (d) Release profiles of AO in water from (a) non-crosslinked and (b) crosslinked (PAH/PAMAM)<sub>7.5</sub> multilayered films. The inset figure in (b) shows the growth of absorbance at 268 nm as a function of the release time. Adapted from ref. 201 with permission from the Royal Society of Chemistry.

Thus, the covalent interlayer linkages and the photochemical crosslinking of the multilayered films encompassing drug reservoirs contributed to the creation of multilayered films with retarded loading-release profiles without compromising the stability, surface morphology and roughness of films. Other authors reported a similar approach for combining post-infiltration, photochemical crosslinking and selective etching to develop porous multilayered films encompassing weak polyelectrolytes.<sup>202–205</sup> Therefore, these systems show great promise in polymer science, since they enable a well-defined control over the film structure, as well as the encapsulation and controlled release of drugs.

Using a similar strategy, Zhang *et al.* prepared a multilayered film comprising DAS crosslinked PAH/PAMAM multilayers, built on a piezoelectric-dielectric flexible film with reduced graphene oxide fillers (rGO-PEI/PVDF-HFP) (Fig. 23a) for improving the release of anti-nausea drugs.<sup>206</sup> These authors observed that the photochemical crosslinking with DAS provided a stable drug matrix while preserving the piezoelectric-dielectric film properties (Fig. 23b). The multilayered film was also assembled on the surface of a disposable gastric lavage tube (Fig. 23c), showcasing that mimetic forces in the same range of human swallowing were transformed by the piezoelectric network into an electrostatic field, leading to an antiemetic drug release increase by 200% within 60 min (Fig. 23d,e). Therefore, the multilayered film can activate electrically triggered releases that were formerly only performed using complicated electrochemical setups and allows the attenuation of nausea, facilitating the intubation process itself. Thus, it is expected that this kind of multilayered platforms could simplify drug applications in various emergent situations and, at the same time, maximize drug release from a matrix, reducing the wasting drugs.

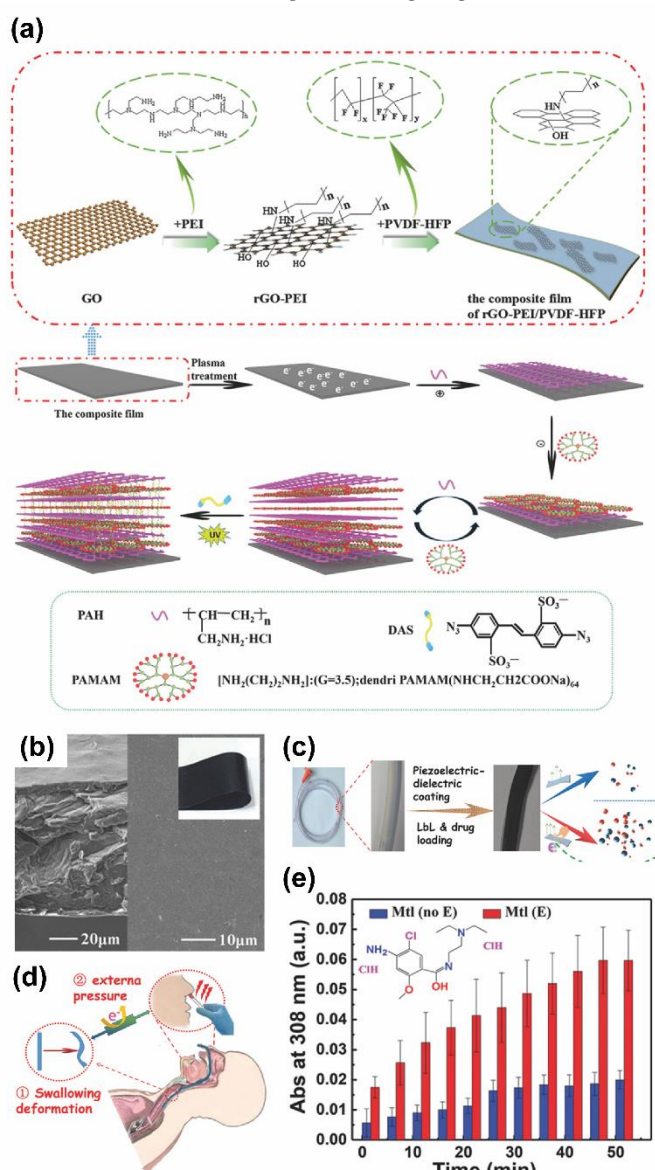


**Fig. 23** (a) Schematic illustration of the preparation of crosslinked PAH/PAMAM LbL films on a piezoelectric-dielectric composite substrate. (b)

SEM image of the cross section of (PAH/PAMAM)<sub>7.5</sub>@rGO-PEI/PVDF-HFP LbL films. The inset figure is a digital photo of the flexible film. (c) Preparation of the multilayers on the disposable gastric lavage tube. (d) Schematic representation of the piezoelectric generation mechanism during the application. (e) Metoclopramide release profiles from (PAH/PAMAM)<sub>10.5</sub>@rGO-PEI/PVDF-HFP LbL films on the disposable gastric lavage tube. Adapted from ref. 206 with permission from the Wiley-VCH Verlag GmbH & Co.

In another example, Oliveira and co-workers reported the fabrication of porous multilayered films incorporating dendrimers and liposomes showcasing their ability to interact with proteins, including bovine serum albumin.<sup>207</sup> Therefore, such films may be useful for releasing ions and small particles from liposomes that will diffuse through the dendrimer's layers.

The design of hollow multilayered microcapsules through the sequential deposition of polymeric materials on the surface of sacrificial colloidal particles, followed by dissolution of the core template, has been attracting growing attention as reservoirs for the encapsulation and on-demand controlled release of drugs/therapeutics.<sup>132,208–210</sup> For instance, PAMAM-loaded LbL microcapsules, through the sequential deposition of PAH and PVS layers onto the surface of calcium carbonate (CaCO<sub>3</sub>) microparticles in which dendrimer is loaded followed by core template dissolution, have been developed (Fig. 24a,b) to study the loading and release of 1-anilinonaphthalene-8-sulfonic acid (ANS) as a model drug.<sup>211</sup> The binding of ANS to the PAMAM dendrimers highly increased the ANS loading in the microcapsules compared to a control lacking PAMAM as seen by a large difference in the fluorescence emission of the dye. The rate of ANS uptake (Fig. 24c) was determined by the rate of transport of ANS across the capsule, while the dissociation of ANS (Fig. 26d) from PAMAM was the rate-determining step for ANS release out of the microcapsules. The reproducibility over the particle size and shape, as well as the versatility in the choice of LbL ingredients for the core-shell capsules constitute an innovative approach to produce modular multilayered microcapsules able to bind and release small molecules.

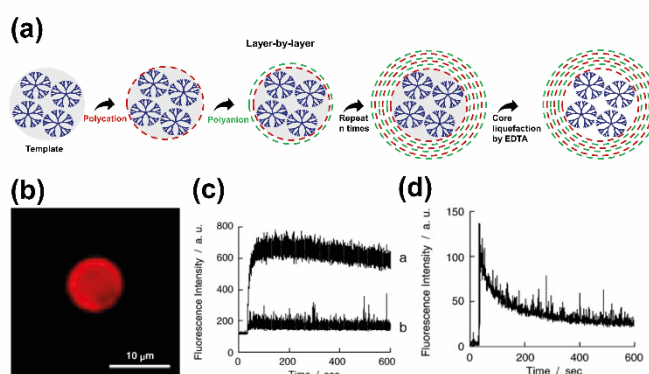


**Fig. 24** (a) Preparation of LbL microcapsules encapsulating dendrimers. The LbL assembly process is developed on CaCO<sub>3</sub> particles, followed by core dissolution to achieve PAMAM-loaded microcapsules. (b) Fluorescence microscope image of PAMAM-loaded PAH/PVS microcapsules, where PAMAM was labeled with tetramethylrhodamine isothiocyanate. (c) ANS uptake into (a) PAMAM-loaded microcapsules and (b) PAMAM-free microcapsules, at pH 4. (d) ANS release profile from PAMAM-loaded microcapsules. b-d: Adapted from ref. 211 with permission from the Elsevier.

Khopade and Caruso developed hollow multilayered microcapsules by coating melamine formaldehyde colloidal particles with

alternating PSS and G4 PAMAM multilayered shells followed by core template dissolution, and evaluated the loading and release profile of the anticancer drug doxorubicin (DOX). It was shown that more than 90% of the loaded DOX was released from the microcapsules after 4–5 h in a 0.154 M NaCl solution.<sup>212</sup> The same authors also studied the adsorption of biological materials, namely cells and proteins on top of the PAMAM/PSS multilayered films adsorbed on the surface of flat substrates and microparticles and modified with PEG-bearing lipids via glutaraldehyde cross-linking, to evaluate the biocompatibility of the multilayered films.<sup>213</sup> It was found that the PEG-modified LbL films reduced the phagocytosis of the microcarriers and adsorption of human serum albumin, as well as their adhesion to the macrophage cell line TPH-1, responsible for granuloma formation and infection at an implant site, when compared to the unmodified LbL films, which prove the biocompatibility of the surface-modified multilayered films. In another study, multilayered microcapsules encompassing *N,N*-disubstituted hydrazine phosphorus-containing dendrimers coupled with oppositely charged linear polyelectrolytes or DNA shells were developed. When compared to the microcapsules developed with solely linear polyelectrolytes, the dendrimer-based microcapsules were found to be much softer, although these microcapsules could be stiffened by the treatment with organic solvents.<sup>214–216</sup> In addition, the effect of the type of surface charges of the multilayered films encompassing either dendrimers and oppositely charged polymers or oppositely charged dendrimers was evaluated on the adhesion and maturation of fetal cortical rat neurons. It was demonstrated that neurons attached preferentially and matured faster in the films having positively charged hydrazine phosphorous dendrimers as the outermost layer (Fig. 25a) when compared with similar films ended in negatively charged ones (Fig. 25b).<sup>115</sup>

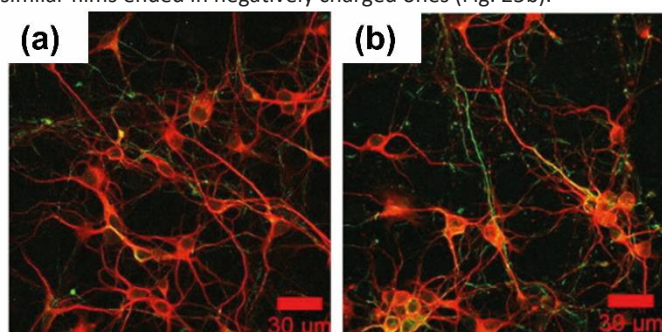


**Fig. 25** Immunofluorescence staining of neurons cultured in film surfaces terminated with (a) positively and (b) negatively charged hydrazine phosphorus dendrimers, after 5 days. Adapted from ref. 115 with permission from the Elsevier.

Polymeric micelles, obtained through the spontaneous arrangement of amphiphilic block copolymers in aqueous solutions, have been appointed as powerful for the encapsulation of poorly water-soluble cancer drugs. As such, the development of polyion complex (PIC) micelles have raised much attention.<sup>217</sup> However, the instability of PIC micelles towards ionic strength under physiological conditions has led researchers to prepare stable PIC micelles by increasing its rigidity through the introduction of dendrimers in their structure.<sup>15,218–220</sup> PIC micelles containing dendritic photosensitizers have been intensively studied in photodynamic therapy (PDT) and as light-harvesting sensitizers (PSS) owing to their optical properties and long triplet excited state lifetime.<sup>221–224</sup> Briefly, this therapeutic approach involves the selective localization of a non-toxic

photoactivatable dye (the PS) in the neoplastic tissue and its irradiation with harmless visible light to generate highly reactive oxygen species that lead to the destruction of the tumor cells.<sup>225</sup> Recently, several approaches have been employed towards the incorporation of PS into new drug delivery systems, which improve the selectivity and efficacy of PDT, as well as reduce the undesirable side effects, such as skin hyperphotosensitivity.<sup>226–228</sup> For instance, Koh and co-workers prepared core-shell LbL nanocapsules encompassing anionic dendrimer porphyrin and cationic PAH multilayered shells on a sacrificial polystyrene template.<sup>229</sup> The resulting capsules revealed high potential for encapsulating DOX for cancer therapy applications. In addition, it was found that the hollow capsules can be used as PS for PDT, whereas the loaded-capsules, after the irradiation, were much more cytotoxic than either chemotherapy or PDT alone, suggesting its application as nano-devices for cancer therapy. As such, the molecular design of dendritic structures can result in the development of innovative and sophisticated multilayered platforms with emergent properties and functions across multiple scale lengths for being used in biomedicine.

### 3.3 Gene therapy

Gene therapy is considered as a powerful approach to prevent and/or treat numerous diseases via the introduction of exogenous DNA into cells. This concept has been broadened and, currently, promising strategies incorporating dendrimers and nucleic acids in multilayered films have been reported. For instance, electrostatically-driven multilayered films composed of G3 amine-terminated poly(disulfide amine) dendronized polymer and oppositely charged plasmid DNA (pDNA) have been proposed for *in vitro* localized gene delivery.<sup>230</sup> Although the disulfide bonds on the polycation are stable during the preparation and storage of the multilayered films, their degradation can be triggered by reductive agents, such as glutathione (GSH). Indeed, the multilayered assemblies were disassembled in the presence of GSH, triggering the release of the complexed DNA, which in turn affected the corresponding gene expression. The G3/DNA multilayered films exhibited good biocompatibility (Fig. 26a), low cytotoxicity (Fig. 26b) and higher transfection levels in comparison with the control encompassing PEI-based DNA multilayered films (Fig. 26c). It was found that the GSH concentration influenced the transfection efficiency of the G3/DNA films in 293T cells. The highest concentrations of GSH tested (5 and 10 mM) accelerated the degradation of the films in small fragments, which promoted the detachment of the adhered cells, leading to low transfection levels. Conversely, the highest transfection activity was obtained in the presence of 2.5 mM GSH (Fig. 26c) with *c.a.* 36% GFP-positive 293T cells after 5 days of co-culture. Therefore, the cleavage of the disulfide bonds in the polycation by the cell attachment on G3/DNA LbL films induced the release of the content into the cytoplasm in a sustained manner. Interestingly, it was found that the pDNA within the G3/DNA multilayered films could be also internalized by 293T cells without any reducing agent because the plasma membrane surface and intracellular environment could trigger the disassembly of the LbL films and release the incorporated pDNA locally. Recently, the focus has been on the synthesis of biodegradable dendrimers,<sup>231</sup> and their incorporation in multilayered assemblies. In particular, the preparation of multilayered films incorporating biodegradable dendrimers and nucleic acids has been on the spotlight. In this regard, Peng *et al.* proposed a completely new approach, highly attractive for gene therapy and tissue engineering owing the ability of the developed multilayered films to control the release of incorporated nucleic acids.<sup>230</sup>

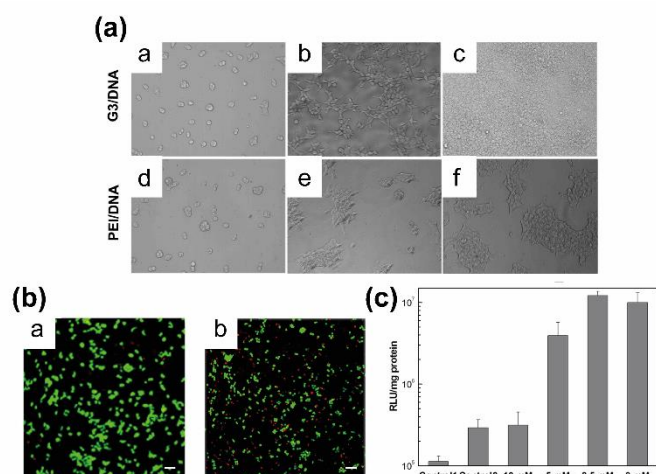


**Fig. 26** (a) Cell attachment and proliferation on the surfaces of (G3/DNA)<sub>9.5</sub> and (PEI/DNA)<sub>9.5</sub> multilayered films for 1 day (a, d), 3 days (b, e) and 5 days (c, f). (b) CLSM images of live (green) and dead (red) 293T cells after 24 h culture on the surfaces of (a) (G3/DNA)<sub>9.5</sub> and (b) (PEI/DNA)<sub>9.5</sub> multilayered films. The scale bar is 5  $\mu$ m. (c) Transfection efficiencies of (G3/DNA)<sub>9.5</sub> multilayered films in 293T cells as a function of the GSH concentration. (PEI/DNA)<sub>9.5</sub> multilayered films were incubated without GSH (shown as control 1), and in 5 mM GSH (shown as control 2). Adapted from ref. 230 with permission from the Elsevier.

Electrospun polymer fibers have been also deeply studied as platforms for the controlled delivery of therapeutics.<sup>232–234</sup> Tomás and co-workers have combined electrospinning and LbL assembly for developing a gene delivery platform for tissue engineering.<sup>235</sup> The biologically active surface was created by surface functionalization of biodegradable electrospun poly(lactic-co-glycolic acid) (PLGA) fibers with chitosan and ALG multilayers (Fig. 27). It was shown that the developed system protects pDNA from endonucleases degradation, serving as a platform for the controlled delivery of pDNA/dendrimer complexes. As such, the attachment, growth, and differentiation of human mesenchymal stem cells towards the osteogenic lineage were supported by the functionalized fiber when a pDNA codifying for human bone morphogenetic protein-2 (hBMP-2) was used. A similar approach has been proposed by Chen *et al.*, who reported the preparation of electrostatic-based multilayered films consisting of cationic PAMAM dendrimers/EGFP-hBMP-2 pDNA complex and anionic naked plasmid on titanium substrates, denoting a great potential to functionalize titanium implants with hBMP-2 gene.<sup>236</sup> Moreover, the multilayered films can be used for the delivery of functional genes in a localized and timely manner at the target site. The gene-functionalized titanium implant improved the osteogenic differentiation of osteoblasts, promoting early bone formation around implant, thus suggesting its possible application in gene-stimulating biomaterials.

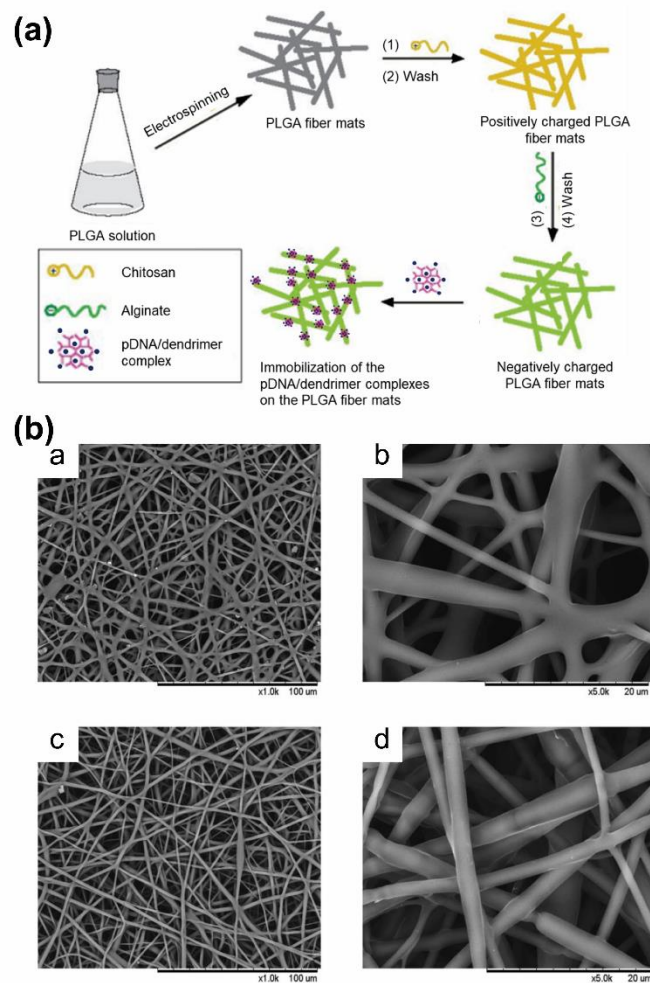


**Fig. 27** (a) Preparation of PLGA fiber mats and immobilization of pDNA/dendrimer complexes in those platforms. Adapted from ref. 234 with permission from the American Chemical Society. (b) SEM images of electrospun PLGA fiber mats (a, b) before and (c, d) after coating with alternating layers of chitosan and ALG. (b) and (d) are magnified images of (a) and (c), respectively. Small pores interconnected are observed in the fiber structure resulting from the electrospinning process. Reprinted from ref. 235 with permission from the Royal Society of Chemistry.

#### 4. Concluding remarks and future perspectives

Dendrimers are very attractive building blocks for a wide array of biomedical, biological and biotechnological applications, such as biosensing, diagnosis, bioimaging, drug/therapeutics delivery, gene therapy, tissue engineering and regenerative medicine owing to their unique and superior structural and physicochemical properties. Those include, their well-defined and highly branched structure, monodisperse and homogeneous 3D globular architecture, multivalency, tunable molecular weight, chemical composition and surface functionality, and precisely controllable nanosize. In this regard, they have been appointed as promising ingredients for the bottom-up assembly of innovative LbL multifunctional systems denoting enhanced structural properties and multifunctionalities not attainable with linear polymers. Those include their intrinsic ability to penetrate the interlayers, produce thicker polymeric multilayered films, and foster stronger interactions between the assembled building blocks. Furthermore, the dendrimer-containing LbL

assemblies provide enhanced binding sites to drugs/therapeutics/bioactive agents either via the internal cores of the dendrimers or their high density of peripheral functional groups, as well as those of the multilayered systems, representing enhanced nanocarriers for the encapsulation, protection, transport and on-demand site-specific and controlled delivery of cargoes.

In this review, we provide a comprehensive overview of the different intermolecular interactions to create dendrimer-containing nanostructured LbL assemblies, including electrostatic interactions, hydrogen bonding, covalent bonding, coordination chemistry, host-guest and biological specific interactions, for bioapplications (Table 1). Although most of the studies reported in the literature focused on the employment of free dendrimers, herein we have shown that there has been an increasing interest in the molecular design and development of supramolecular dendrimer-based multilayered assemblies for addressing multiple biological and biomedical applications, including biosensing, bioimaging, drug/therapeutics delivery, and gene therapy. This has been fueled by the simplicity, cost-effectiveness, mild processing conditions, and high versatility imparted by the LbL assembly technology in terms of the unprecedented choice of both inanimate and animate substrates to be coated and building blocks to be assembled via a multitude of intermolecular interactions and assembly methodologies. In fact, the LbL technology enables shaping a wide array of innovative and highly controlled multifunctional bioarchitectures, ranging from simple to more complex and elaborated structures spanning from the zero- (0D) to the third dimension (3D), not attainable with LbL-free dendrimers. The integration of dendrimers as ingredients in LbL assemblies enables processing them not only into core-shell particles and hollow multilayered capsules or tubes, but also into multilayered thin films, free-standing membranes, among others depending on the template to be coated and envisioned bioapplication. Besides, the adaptable and tunable chemistry denoted by the dendrimers turn them into promising nanoreservoirs for enabling high payload carrying and controlled release at a target specific site. In addition, the multivalency assigned by the high density of surface functional groups allows tethering targeting-specific cargoes or ligands in a precise controllable manner for improving their biocompatibility, site-specific controlled delivery, circulation time in the bloodstream and readily interact with the cell membrane via the cell specific receptors. Although these features are commonly exploited in LbL-free dendrimers, the integration of dendrimers into LbL systems allows an enhanced protection of themselves and their cargo from undesirable interactions with the biological environment and improve the aqueous solubility and biodistribution of the cargo with reduced side effects. Moreover, the LbL architecture itself could be easily modulated and imparted with stimuli-responsive materials, thus rendering the LbL systems smart systems for on-demand site-specific sustained delivery of dendrimer and encapsulated cargoes. As such, there is no doubt that the development of supramolecular dendrimer-containing multilayered systems is highly beneficial when compared to the LbL-free dendrimers and LbL ensembles prepared with linear polymers.

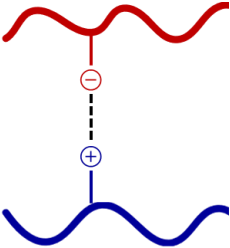
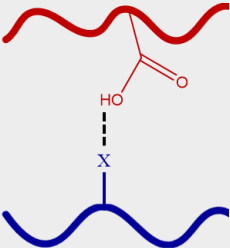
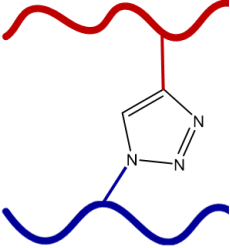
However, despite the benefits and significance of the developed dendrimer-based multifunctional LbL systems for bioapplications, there are still major bottlenecks that inhibit their translation into practical clinical applications. Among them, most of the higher generation dendrimers assembled into LbL systems are cationic, thus raising cytotoxicity concerns and biological cell membrane disruption. This drawback ought to be addressed by the LbL community by taking advantage of the already successfully

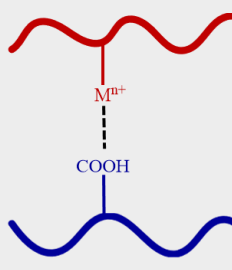
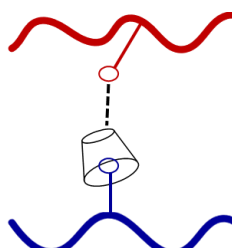
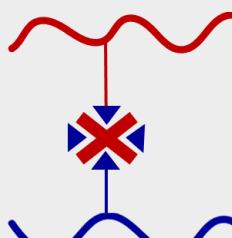
functionalized amine-ended dendrimers with PEG, natural saccharides, or other ligands. Furthermore, a major hurdle pertains to the nonbiodegradability of the mostly used and LbL assembled dendrimers under biologically relevant conditions, which elicit cytotoxicity effects by transposing the cell membrane and accumulating intracellularly. In this regard, biodegradable dendrimers have been gathering much interest and hold great promise as smart nanocarriers for bioapplications, including for on-demand cell-regulated intracellularly controlled and sustained therapeutics delivery and tissue regeneration. For this purpose, the use of biorthogonal coupling reactions, namely the strain-promoted azide-alkyne cycloaddition or thiol-ene, among others, represents a powerful strategy for the synthesis and covalent decoration of dendrimers in the absence of metal catalysts, additives and organic solvents.<sup>149</sup> The possibility of developing biocompatible and biodegradable smart dendrimer-containing LbL nanoassemblies is particularly attractive for the nanoencapsulation of living cells, aiming to protect them and their cargo from extreme conditions in the biological environment and enable their on-demand delivery at the target site. Furthermore, those smart biocompatible and biodegradable nanoassemblies also open new pathways in coating core-shell particles and produce hollow multilayered nano/micro-capsules able to bind and release payloads on-demand and be used for cellular uptake. In this regard, the choice of the materials to be assembled into multilayered nanoassemblies dictate their final end-use. For instance, the multilayered nanoshells of hollow nano/micro-capsules could be enlisted with “intelligent” ingredients, i.e. materials that are (multi)stimuli-responsive (e.g., pH-, temperature-, ionic strength-, light-sensitive, among others), whose response can be modulated by playing with stimuli. An illustrative example pertains to the development of hollow nanocapsules entailing pH-sensitive multilayered shells that would be stable under physiological conditions and after being internalized by cells and reaching the endosomes, denoting a slightly acidic pH, would be degraded and release the encapsulated bioactive agents. Besides, we envisage that the possibility of using biocompatible and biodegradable dendrimers as own nanocarrier vehicles and coating them with stimuli-responsive LbL nanoshells constitutes an innovative approach that would afford them with superior performance and improved control at the nanoscale tackling a diverse set of bioapplications.

Of great interest is also the capacity to accelerate the production and scale-up of dendrimers, with novel strategies and reactions challenging the conventionally tedious stepwise synthesis of dendrimers.<sup>237</sup> The noncovalent synthesis of dendrimers by the self-assembly of small amphiphilic dendrimer building units is a revolutionary approach for bioapplications, being able to mimic the covalently developed dendrimers in their structure and functions.<sup>238</sup> Furthermore, we envision that the integration of the bottom-up LbL assembly technology with other prominent nano- and micro-fabrication methodologies, including photolithography, photopatterning and 3D bioprinting, holds great promise for tailoring the construction of functional, stable and well-defined nanostructures. Moreover, it would also enable the design of complex, sophisticated and multiscale devices exhibiting emergent properties and multifunctionalities. Those include adaptive, bioinspired and multi-stimuli responsive behavior, as well as self-healing ability, thus opening new avenues to increase the potentialities and the range of applications of those structures. In summary, although the incorporation of dendrimers in nanostructured LbL assemblies has raised increasing attention, there is still plenty of room for further development and innovation, and

challenges that ought to be addressed while the field is expanding to construct advanced and sophisticated devices for diverse applications in the biological and biomedical fields. Therefore, we foresee that this review will provide a fresh perspective and stimulate the scientific community in exploiting the unique features of both dendrimers and LbL assembly technology and contribute towards accelerating the development and clinical translation of dendrimer-based multifunctional supramolecular multilayered nanoassemblies.

**Table 1.** Intermolecular interactions driving the LbL assembly of dendrimer-containing LbL nanoassemblies and their corresponding main features and bioapplications.

ARTICLE	Journal Name			
Intermolecular Interactions	Main features	Dendrimer-based LbL nanoassemblies	Bioapplications	Representative references
<p data-bbox="97 293 260 353"><b>Electrostatic Interactions</b></p> 	<ul style="list-style-type: none"> <li>• The most explored mechanism to develop dendrimer-containing multilayered assemblies</li> <li>• The LbL assembly process can be performed with virtually any charged and water-soluble molecules</li> <li>• The structure, composition and properties of the multilayered assemblies can be precisely tailored by adjusting several parameters (<i>e.g.</i>, pH, ionic strength, polymer molecular weight)</li> </ul>	<ul style="list-style-type: none"> <li>• Core-shell particles</li> <li>• Multilayered thin films</li> <li>• Robust free-standing multilayered membranes</li> <li>• Hollow multilayered capsules</li> </ul>	<ul style="list-style-type: none"> <li>• Biosensing</li> <li>• Diagnostics</li> <li>• Drug/therapeutics delivery</li> <li>• Cancer therapy</li> <li>• Gene therapy</li> <li>• Tissue engineering</li> </ul>	<p>83, 108-116, 119-123, 128, 174, 182, 196, 199, 211, 212, 229, 230, 235, 236</p>
<p data-bbox="113 857 244 918"><b>Hydrogen Bonding</b></p> 	<ul style="list-style-type: none"> <li>• Enables the incorporation of charged and uncharged molecules within the multilayers</li> <li>• Fabrication of more stable and robust films than the ones developed by electrostatic interactions</li> <li>• The LbL films growth by assembling polymers bearing moieties that can act as hydrogen bonding donors and hydrogen bonding acceptors and can be accomplished in aqueous solutions or in organic solvents</li> <li>• The LbL films created using hydrogen bonding are highly sensitive to pH</li> </ul>	<ul style="list-style-type: none"> <li>• Single component multilayered thin films</li> <li>• Multilayered thin films relying on different components</li> </ul>	<ul style="list-style-type: none"> <li>• Drug/therapeutics delivery</li> <li>• Biosensing</li> </ul>	<p>130-134, 137-139</p>
<p data-bbox="65 1563 292 1592"><b>Covalent Bonding</b></p> 	<ul style="list-style-type: none"> <li>• Flexibility in the selection of the molecules to be assembled, allowing the development of multifunctional assemblies that cannot be prepared by electrostatic-driven LbL assembly methods</li> <li>• Fabrication of more stable and robust multilayered films than the ones developed by electrostatic interactions and hydrogen bonding</li> <li>• The exposure of multilayered films to UV irradiation induces changes in the properties of the films, increasing their robustness and stability</li> <li>• The design of stimuli-responsive multilayers is not appropriate due to the irreversibility of the covalent-based systems</li> </ul>	<ul style="list-style-type: none"> <li>• Multilayered thin films</li> <li>• Hollow multilayered capsules</li> </ul>	<ul style="list-style-type: none"> <li>• Immunoprotection</li> <li>• Biosensing</li> <li>• Drug/therapeutics delivery</li> </ul>	<p>140, 141, 144-146, 153-155, 175, 201</p>

<p><b>Coordination Chemistry Interactions</b></p> 	<ul style="list-style-type: none"> <li>• Design of well-ordered, stable and highly oriented multilayered films encompassing organic ligands and transition metal ions</li> <li>• Enables the control over surface structure at the molecular level</li> </ul>	<ul style="list-style-type: none"> <li>• Multilayered thin films</li> </ul>	<ul style="list-style-type: none"> <li>• Biosensing</li> </ul>	65, 83, 156, 157
<p><b>Host-Guest Interactions</b></p> 	<ul style="list-style-type: none"> <li>• Preparation of multilayered films based on highly selective and strong interactions between host and guest molecules</li> </ul>	<ul style="list-style-type: none"> <li>• Multilayered thin films</li> </ul>	<ul style="list-style-type: none"> <li>• Electronic and optical devices</li> </ul>	158-161
<p><b>Biologically Specific Interactions</b></p> 	<ul style="list-style-type: none"> <li>• Development of LbL assemblies with high specificity and functionality to the target molecules</li> <li>• Encompass specific biological interactions (e.g., avidin-biotin, DNA hybridization)</li> <li>• Polymers with the same charge can be assembly within the multilayers provided that they entail complementary biospecific interactions</li> </ul>	<ul style="list-style-type: none"> <li>• Multilayered thin films</li> <li>• Hollow multilayered capsules</li> </ul>	<ul style="list-style-type: none"> <li>• Biosensors</li> <li>• Diagnostics</li> <li>• Molecular biology</li> </ul>	162-168

**Note:** The schematic illustrations represent dendrimer-polymer and dendrimer-dendrimer (in the case of the electrostatic interactions and hydrogen bonding) interactions.

## Conflicts of interest

There are no conflicts to declare.

## Acknowledgements

This work was supported by the Marine Biotechnology ERA-NET project "BLUETEETH" (ERA-MBT/0002/2015) funded by the Portuguese Foundation for Science and Technology (FCT) under EU FP7 (Grant Agreement number: 604814), as well as by the Programa Operacional Regional do Centro – Centro 2020, in the component FEDER, and by national funds (OE) through FCT/MCTES, in the scope of the project "SUPRASORT" (PTDC/QUI-OUT/30658/2017, CENTRO-01-0145-FEDER-030658). This work was developed within the scope of the project CICECO – Aveiro Institute of Materials, UIDB/50011/2020 & UIDP/50011/2020, financed by national funds through the FCT/MCTES. Financial aid was also obtained from the Spanish Ministry of Science and Innovation (RTI2018-102212-B-I00), the Xunta de Galicia (ED431C 2018/30, and Centro singular de

investigación de Galicia accreditation 2019-2022, ED431G2019/03), Axencia Galega de Innovación (IN845D 2020/09), and the European Union (European Regional Development Fund-ERDF). Cristiana Sousa and João Borges gratefully acknowledge the financial support by FCT through the individual PhD grant (2020.04408.BD) and individual Assistant Researcher contract (2020.00758.CEECIND) under the Scientific Employment Stimulus – Individual Call, respectively.

## References

- 1 D. Astruc, E. Boisselier and C. Ornelas, *Chem. Rev.*, 2010, **110**, 1857-1959. doi:10.1021/cr900327d.
- 2 A. M. Caminade, C. O. Turrin, R. Laurent, A. Ouali and B. Delavaux-Nicot, *Dendrimers: towards catalytic, material and biomedical uses*, John Wiley & Sons, UK, 2011.
- 3 D. A. Tomalia and S. N. Khanna, *Chem. Rev.*, 2016, **116**, 2705-2774. doi:10.1021/acs.chemrev.5b00367.

- 4 B. N. S. Thota, L. H. Urner and R. Haag, *Chem. Rev.*, 2016, **116**, 2079-2102. doi:10.1021/acs.chemrev.5b00417.
- 5 C. C. Lee, J. A. MacKay, J. M. J. Fréchet and F. C. Szoka, *Nat. Biotechnol.*, 2005, **23**, 1517-1526. doi:10.1038/nbt1171.
- 6 D. A. Tomalia, *Prog. Polym. Sci.*, 2005, **30**, 294-324. doi:10.1016/j.progpolymsci.2005.01.007.
- 7 B. Helms and E. W. Meijer, *Science*, 2006, **313**, 929-930. doi:10.1126/science.1130639.
- 8 M. A. Mintzer and M. W. Grinstaff, *Chem. Soc. Rev.*, 2011, **40**, 173-190. doi:10.1039/b901839p.
- 9 B. Noriega-Luna, L. A. Godínez, F. J. Rodríguez, A. Rodríguez, G. Z. L. de Larrea, C. F. Sosa-Ferreyra, R. F. Mercado-Curiel, J. Manríquez and E. Bustos, *J. Nanomater.*, 2014, **2014**. doi:10.1155/2014/507273.
- 10 X. Yang, H. Shang, C. Ding and J. Li, *Polym. Chem.*, 2015, **6**, 668-680. doi:10.1039/c4py01537a.
- 11 D. R. Sikwal, R. S. Kalhapure and T. Govender, *Eur. J. Pharm. Sci.*, 2017, **97**, 113-134. doi:10.1016/j.ejps.2016.11.013.
- 12 S. Mignani, J. Rodrigues, H. Tomas, M. Zablocka, X. Shi, A. M. Caminade, J. P. Majoral, *Chem. Soc. Rev.*, 2018, **47**, 514-532. doi:10.1039/c7cs00550d.
- 13 M. Ghaffari, G. Dehghan, F. Abedi-Gaballu, S. Kashanian, B. Baradaran, J. E. N. Dolatabadi, D. Losic, *Eur. J. Pharm. Sci.*, 2018, **122**, 311-330. doi:10.1016/j.ejps.2018.07.020.
- 14 U. Boas and P. M. H. Heegaard, *Chem. Soc. Rev.*, 2004, **33**, 43-63. doi:10.1039/b309043b.
- 15 N. Nishiyama, W. D. Jang and K. Kataoka, *New J. Chem.*, 2007, **31**, 1074-1082. doi:10.1039/b616050f.
- 16 Svenson S, *Eur. J. Pharm. Biopharm.*, 2009, **71**, 445-462. doi:10.1016/j.ejpb.2008.09.023.
- 17 A. R. Menjoge, R. M. Kannan and D. A. Tomalia, *Drug Discov. Today*, 2010, **15**, 171-185. doi:10.1016/j.drudis.2010.01.009.
- 18 M. de La Fuente, M. Raviña, A. Sousa-Herves, J. Correa, R. Riguera, E. Fernandez-Megia, A. Sánchez and M. J. Alonso, *Nanomedicine*, 2012, **7**, 1667-1681. doi:10.2217/nnm.12.51.
- 19 P. Kesharwani, K. Jain and N. K. Jain, *Prog. Polym. Sci.*, 2014, **39**, 268-307. doi:10.1016/j.progpolymsci.2013.07.005.
- 20 M. C. Lukowiak, B. N. S. Thota and R. Haag, *Biotechnol. Adv.*, 2015, **33**, 1327-1341. doi:10.1016/j.biotechadv.2015.03.014.
- 21 F. Abedi-Gaballu, G. Dehghan, M. Ghaffari, R. Yekta, S. Abbaspour-Ravasjani, B. Baradaran, J. E. N. Dolatabadi and M. R. Hamblin, *Appl. Mater. Today*, 2018, **12**, 177-190. doi:10.1016/j.apmt.2018.05.002.
- 22 C. Song, M. Shen, J. Rodrigues, S. Mignani, J. P. Majoral and X. Shi, *Coord. Chem. Rev.*, 2020, **421**, 213463. doi:10.1016/j.ccr.2020.213463.
- 23 L. Zhang, D. Shi, Y. Gao, T. Zhou and M. Chen, *Polym. Chem.*, 2020, **11**, 2252-2261. doi:10.1039/d0py00008f.
- 24 O. P. Perumal, R. Inapagolla, S. Kannan and R. M. Kannan, *Biomaterials*, 2008, **29**, 3469-3476. doi:10.1016/j.biomaterials.2008.04.038.
- 25 L. Albertazzi, M. Serresi, A. Albanese and F. Beltram, *Mol. Pharm.*, 2010, **7**, 680-688. doi:10.1021/mp9002464.
- 26 L. Albertazzi, M. Fernandez-Villamarín, R. Riguera and E. Fernandez-Megia, *Bioconjug. Chem.*, 2012, **23**, 1059-1068. doi:10.1021/bc300079h.
- 27 E. Nikolskaya, N. Yabbarov, O. Zhunina, O. Tereshenko, M. Mollaev, M. Faustova, I. Zamulaeva and E. Severin, *Mater. Today Proc.*, 2017, **4**, 6849-6855. doi:10.1016/j.matpr.2017.07.013.
- 28 H. Hosseinkhani, W. J. He, C. H. Chiang, P. D. Hong, D. S. Yu, A. J. Domb and K. L. Ou, *J. Nanoparticle Res.*, 2013, **15**, 1794. doi:10.1007/s11051-013-1794-z.
- 29 H. Yin, R. L. Kanasty, A. A. Eltoukhy, A. J. Vegas, J. R. Dorkin and D. G. Anderson, *Nat. Rev. Genet.*, 2014, **15**, 541-555. doi:10.1038/nrg3763.
- 30 J. A. Kretzmann, C. W. Evans, M. Norret and K. S. Iyer, in *Comprehensive Supramolecular Chemistry II*, ed. G. W. Gokel and L. Barbour, Academic Press, UK, 2017, pp. 237-256.
- 31 M. Guillot-Nieckowski, S. Eisler and F. Diederich, *New J. Chem.*, 2007, **31**, 1111-1127. doi:10.1039/b614877h.
- 32 Y. Wang, X. Cao, R. Guo, M. Shen, M. Zhang, M. Zhu and X. Shi, *Polym. Chem.*, 2011, **2**, 1754-1760. doi:10.1039/c1py00179e.
- 33 C. Zhang, D. Pan, K. Luo, N. Li, C. Guo, X. Zheng and Z. Gu, *Polym. Chem.*, 2014, **5**, 5227-5235. doi:10.1039/c4py00601a.
- 34 Z. Zhang, Y. Zhou, Z. Zhou, Y. Piao, N. Kalva, X. Liu, J. Tang and Y. Shen, *Polym. Chem.*, 2018, **9**, 438-449. doi:10.1039/c7py01492a.
- 35 M. Ye, Y. Qian, J. Tang, H. Hu, M. Sui and Y. Shen, *J. Control. Release*, 2013, **169**, 239-245. doi:10.1016/j.jconrel.2013.01.034.
- 36 J. Tang, Y. Sheng, H. Hu and Y. Shen, *Prog. Polym. Sci.*, 2013, **38**, 462-502. doi:10.1016/j.progpolymsci.2012.07.001.
- 37 Y. Chang, Y. Li, X. Meng, N. Liu, D. Sun, H. Liu and J. Wang, *Polym. Chem.*, 2013, **4**, 789-794. doi:10.1039/c2py20740k.
- 38 Z. Qiao and X. Shi, *Prog. Polym. Sci.*, 2015, **44**, 1-27. doi:10.1016/j.progpolymsci.2014.08.002.
- 39 F. Liko, F. Hindré and E. Fernandez-Megia, *Biomacromolecules*, 2016, **17**, 3103-3114. doi:10.1021/acs.biomac.6b00929.

- 40 Y. Fan, J. Zhang, M. Shi, D. Li, C. Lu, X. Cao, C. Peng, S. Mignani, J. P. Majoral and X. Shi, *Nano Lett.*, 2019, **19**, 1216-1226. doi:10.1021/acs.nanolett.8b04757.
- 41 Y. Fan, W. Tu, M. Shen, X. Chen, Y. Ning, J. Li, T. Chen, H. Wang, F. Yin, Y. Liu, et al., *Adv. Funct. Mater.*, 2020, **30**, 1909285. doi:10.1002/adfm.201909285.
- 42 P. N. Desai, Q. Yuan and H. Yang, *Biomacromolecules*, 2010, **11**, 666-673. doi:10.1021/bm901240g.
- 43 J. Satija, V. V. R. Sai and S. Mukherji, *J. Mater. Chem.*, 2011, **21**, 14367-14386. doi:10.1039/c1jm10527b.
- 44 G. Tang, S. S. Y. Chen, P. E. Shaw, K. Hegedus, X. Wang, P. L. Burn and P. Meredith, *Polym. Chem.*, 2011, **2**, 2360-2368. doi:10.1039/c1py00222h.
- 45 M. Hasanzadeh, N. Shadjou, M. Eskandani, J. Soleymani, F. Jafari and M. de la Guardia, *TrAC- Trends Anal. Chem.*, 2014, **53**, 137-149. doi:10.1016/j.trac.2013.09.015.
- 46 N. Joshi and M. Grinstaff, *Curr. Top. Med. Chem.*, 2008, **8**, 1225-1236. doi:10.2174/156802608785849067.
- 47 J. M. Oliveira, R. A. Sousa, N. Kotobuki, M. Tadokoro, M. Hirose, J. F. Mano, *Biomaterials*, 2009, **30**, 804-813. doi:10.1016/j.biomaterials.2008.10.024.
- 48 J. M. Oliveira, A. J. Salgado, N. Sousa, J. F. Mano and R. L. Reis, *Prog. Polym. Sci.*, 2010, **35**, 1163-1194. doi:10.1016/j.progpolymsci.2010.04.006.
- 49 J. M. Oliveira, N. Kotobuki, M. Tadokoro, M. Hirose, J. F. Mano, R. L. Reis and H. Ohgushi, *Bone*, 2010, **46**, 1424-1435. doi:10.1016/j.bone.2010.02.007.
- 50 B. Gorain, M. Tekade, P. Kesharwani, A. K. Iyer, K. Kalia and R. K. Tekade, *Drug Discov. Today*, 2017, **22**, 652-664. doi:10.1016/j.drudis.2016.12.007.
- 51 M. Komath, H. K. Varma, A. John, V. Krishnan, D. Simon, M. Ramanathan and G. S. Bhuvaneshwar, in *Regenerative Medicine: Laboratory to Clinic*, ed. A. Mukhopadhyay, Springer, Singapore, 2017, pp. 423-447.
- 52 P. R. Dash, M. L. Read, L. B. Barrett, M. A. Wolfer and L. W. Seymour, *Gene Ther.*, 1999, **6**, 643-650. doi:10.1038/sj.gt.3300843.
- 53 C. M. Wiethoff and C. R. Middaugh, *J. Pharm. Sci.*, 2003, **92**, 203-217. doi:10.1002/jps.10286.
- 54 Y. Cheng, L. Zhao, Y. Li and T. Xu, *Chem. Soc. Rev.*, 2011, **40**, 2673-2703. doi:10.1039/c0cs00097c.
- 55 C. H. Jones, C. K. Chen, A. Ravikrishnan, S. Rane and B. A. Pfeifer, *Mol. Pharm.*, 2013, **10**, 4082-4098. doi:10.1021/mp400467x.
- 56 A. P. Pêgo, H. Oliveira and P. M. Moreno, in *Drug Delivery Systems: Advanced Technologies Potentially Applicable in Personalised Treatment*, ed. J. Coelho, Springer, Dordrecht, 2013, pp. 185-224.
- 57 K. Luo, B. He, Y. Wu, Y. Shen and Z. Gu, *Biotechnol. Adv.*, 2014, **32**, 818-830. doi:10.1016/j.biotechadv.2013.12.008.
- 58 Y. Kim, E. J. Park and D. H. Na, *Arch. Pharm. Res.*, 2018, **41**, 571-582. doi:10.1007/s12272-018-1008-4.
- 59 D. Lombardo, P. Calandra, L. Pasqua and S. Magazù, *Materials*, 2020, **13**, 1048. doi:10.3390/ma13051048.
- 60 A. A. Chis, C. Dobrea, C. Morgovan, A. M. Arseniu, L. L. Rus, A. Butuca, A. M. Juncan, M. Totan, A. L. Vonica-Tincu, G. Cormos, et al., *Molecules*, 2020, **25**, 3982. doi:10.3390/molecules25173982.
- 61 K. Jain, P. Kesharwani, U. Gupta and N. K. Jain, *Int. J. Pharm.*, 2010, **394**, 122-142. doi:10.1016/j.ijpharm.2010.04.027.
- 62 L. J. Fox, R. M. Richardson and W. H. Briscoe, *Adv. Colloid Interface Sci.*, 2018, **257**, 1-18. doi:10.1016/j.cis.2018.06.005.
- 63 A. Janaszewska, J. Lazniewska, P. Trzepiński, M. Marcinkowska and B. Klajnert-Maculewicz, *Biomolecules*, 2019, **9**, 330. doi:10.3390/biom9080330.
- 64 M. Pooresmaeil and H. Namazi, *Eur. Polym. J.*, 2021, **148**, 110356. doi:10.1016/j.eurpolymj.2021.110356.
- 65 S. Watanabe and S. L. Regen, *J. Am. Chem. Soc.*, 1994, **116**, 8855-8856. doi:10.1021/ja00098a074.
- 66 R. K. Iler, *J. Colloid Interface Sci.*, 1966, **21**, 569-594. doi:10.1016/0095-8522(66)90018-3.
- 67 G. Decher and J. D. Hong, *Makromol. Chem. Macromol. Symp.*, 1991, **46**, 321-327. doi:10.1002/masy.19910460145.
- 68 G. Decher and J. D. Hong, *Ber. Bunsenges Phys. Chem.*, 1991, **95**, 1430-1434. doi:10.1002/bbpc.19910951122.
- 69 G. Decher, J. D. Hong and J. Schmitt, *Thin Solid Films*, 1992, **210**, 831-835. doi:10.1016/0040-6090(92)90417-A.
- 70 Y. Lvov, G. Decher and H. Möhwald, *Langmuir*, 1993, **9**, 481-486. doi:10.1021/la00026a020.
- 71 G. Decher, *Science*, 1997, **277**, 1232-1237. doi:10.1126/science.277.5330.1232.
- 72 K. Ariga, Y. Yamauchi, G. Ryzdek, Q. Ji, Y. Yonamine, K. C. W. Wu and J. P. Hill, *Chem. Lett.*, 2014, **43**, 36-68. doi:10.1246/cl.130987.
- 73 Y. Wang, A. S. Angelatos and F. Caruso, *Chem. Mater.*, 2008, **20**, 848-858. doi:10.1021/cm7024813.
- 74 F. X. Xiao, M. Pagliaro, Y. J. Xu and B. Liu, *Chem. Soc. Rev.*, 2016, **45**, 3088-3121. doi:10.1039/c5cs00781j.
- 75 P. Sher, C. A. Custódio and J. F. Mano, *Small*, 2010, **6**, 2644-2648. doi:10.1002/smll.201001066.
- 76 M. Lee, W. Park, C. Chung, J. Lim, S. Kwon, K. H. Ahn, S. J. Lee and K. Char, *Lab Chip*, 2010, **10**, 1160-1166. doi:10.1039/b919753b.
- 77 J. P. DeRocher, P. Mao, J. Han, M. F. Rubner and R. E. Cohen,

- Macromolecules*, 2010, **43**, 2430-2437. doi:10.1021/ma902451s.
- 78 Y. Li, X. Wang and J. Sun, *Chem. Soc. Rev.*, 2012, **41**, 5998-6009. doi:10.1039/c2cs35107b.
- 79 J. J. Richardson, D. Teng, M. Björnmalm, S. T. Gunawan, J. Guo, J. Cui, G. V. Franks and F. Caruso, *Langmuir*, 2014, **30**, 10028-10034. doi:10.1021/la502176g.
- 80 J. Cui, M. P. van Koevorden, M. Müllner, K. Kempe and F. Caruso, *Adv. Colloid Interface Sci.*, 2014, **207**, 14-31. doi:10.1016/j.cis.2013.10.012.
- 81 J. J. Richardson, M. Björnmalm and F. Caruso, *Science*, 2015, **348**, aaa2491. doi:10.1126/science.aaa2491.
- 82 J. J. Richardson, J. Cui, M. Björnmalm, J. A. Braunger, H. Ejima and F. Caruso, *Chem. Rev.*, 2016, **116**, 14828-14867. doi:10.1021/acs.chemrev.6b00627.
- 83 J. Borges and J. F. Mano, *Chem. Rev.*, 2014, **114**, 8883-8942. doi:10.1021/cr400531v.
- 84 Y. Lvov, H. Haas, G. Decher, H. Möhwald, A. Mikhailov, B. Mtchedlishvily, E. Morgunova and B. Vainshtein, *Langmuir*, 1994, **10**, 4232-4236. doi:10.1021/la00023a052.
- 85 S. W. Keller, H. N. Kim and T. E. Mallouk, *J. Am. Chem. Soc.*, 1994, **116**, 8817-8818. doi:10.1021/ja00098a055.
- 86 Y. Lvov, K. Ariga and T. Kunitake, *Chem. Lett.*, 1994, **23**, 2323-2326. doi:10.1246/cl.1994.2323.
- 87 Z. Tang, Y. Wang, P. Podsiadlo and N. A. Kotov, *Adv. Mater.*, 2006, **18**, 3203-3224. doi:10.1002/adma.200600113.
- 88 K. T. Nam, D. W. Kim, P. J. Yoo, C. Y. Chiang, N. Meethong, P. T. Hammond, Y. M. Chiang and A. M. Belcher, *Science*, 2006, **312**, 885-888. doi:10.1126/science.1122716.
- 89 K. Ariga, J. P. Hill and Q. Ji, *Phys. Chem. Chem. Phys.*, 2007, **9**, 2319-2340. doi:10.1039/b700410a.
- 90 J. Han, D. Yan, W. Shi, J. Ma, H. Yan, M. Wei, D. G. Evans and X. Duan, *J. Phys. Chem. B*, 2010, **114**, 5678-5685. doi:10.1021/jp9114018.
- 91 C. W. Chiu and J. J. Lin, *Prog. Polym. Sci.*, 2012, **37**, 406-444. doi:10.1016/j.progpolymsci.2011.07.007.
- 92 S. M. Oliveira, T. H. Silva, R. L. Reis and J. F. Mano, *J. Mater. Chem. B*, 2013, **1**, 4406-4418. doi:10.1039/c3tb20624f.
- 93 J. Borges, J. M. Campiña and A. F. Silva, *J. Mater. Chem. B*, 2013, **1**, 500-511. doi:10.1039/c3tb00115b.
- 94 E. V. Skorb and D. V. Andreeva, *Polym. Chem.*, 2013, **4**, 4834-4845. doi:10.1039/c3py00088e.
- 95 J. Borges, L. C. Rodrigues, R. L. Reis and J. F. Mano, *Adv. Funct. Mater.*, 2014, **24**, 5624-5648. doi:10.1002/adfm.201401050.
- 96 R. R. Costa, M. Alatorre-Meda and J. F. Mano, *Biotechnol. Adv.*, 2015, **33**, 1310-1326. doi:10.1016/j.biotechadv.2015.04.005.
- 97 J. M. Silva, R. L. Reis and J. F. Mano, *Small*, 2016, **12**, 4308-4342. doi:10.1002/smll.201601355.
- 98 S. Jin, H. Gu, X. Chen, X. Liu, W. Zhan, T. Wei, X. Sun, C. Ren and H. Chen, *Colloids Surfaces B Biointerfaces*, 2018, **167**, 28-35. doi:10.1016/j.colsurfb.2018.03.047.
- 99 X. Zhang, Y. Xu, X. Zhang, H. Wu, J. Shen, R. Chen, Y. Xiong, J. Li and S. Guo, *Prog. Polym. Sci.*, 2019, **89**, 76-107. doi:10.1016/j.progpolymsci.2018.10.002.
- 100 K. f. Ren, M. Hu, H. Zhang, B. c. Li, W. x. Lei, J. y. Chen, H. Chang, L. m. Wang and J. Ji, *Prog. Polym. Sci.*, 2019, **92**, 1-34. doi:10.1016/j.progpolymsci.2019.02.004.
- 101 S. V. Kononova, E. V. Kruchinina, V. A. Petrova, Y. G. Baklagina, V. V. Klechkovskaya, A. S. Orekhov, E. N. Vlasova, E. N. Popova, G. N. Gubanov and Y. A. Skorik, *Carbohydr. Polym.*, 2019, **209**, 10-19. doi:10.1016/j.carbpol.2019.01.003.
- 102 R. R. Costa and J. F. Mano, *Chem. Soc. Rev.*, 2014, **43**, 3453-3479. doi:10.1039/c3cs60393h.
- 103 S. Park, U. Han, D. Choi and J. Hong, *Biomater. Res.*, 2018, **22**, 29. doi:10.1186/s40824-018-0139-5.
- 104 D. Alkekhaia, P. T. Hammond and A. Shukla, *Annu. Rev. Biomed. Eng.*, 2020, **22**, 1-24. doi: 10.1146/annurev-bioeng060418-052350.
- 105 M. H. Park, S. S. Agasti, B. Creran, C. Kim and V. M. Rotello, *Adv. Mater.*, 2011, **23**, 2839-2842. doi:10.1002/adma.201004409.
- 106 K. Sato and J. I. Anzai, *Molecules*, 2013, **18**, 8440-8460. doi:10.3390/molecules18078440.
- 107 M. Ujihara and T. Imae, *Polym. Int.*, 2010, **59**, 37-144. doi:10.1002/pi.2713.
- 108 J. Zeng and M. Matsusaki, *Polym. Chem.*, 2019, **10**, 2960-2974. doi:10.1039/c9py00305c.
- 109 J. L. Casson, H. L. Wang, J. B. Roberts, A. N. Parikh, J. M. Robinson and M. S. Jhal, *J. Phys. Chem. B*, 2002, **106**, 1697-1702. doi:10.1021/jp012526r.
- 110 B. Y. Kim and M. L. Bruening, *Langmuir*, 2003, **19**, 94-99. doi:10.1021/la026353o.
- 111 C. Li, K. Mitamura and T. Imae, *Macromolecules*, 2003, **36**, 9957-9965. doi:10.1021/ma035138r.
- 112 F. N. Crespilho, F. Huguenin, V. Zucolotto, P. Olivi, F. C. Nart and O. N. Oliveira, *Electrochem. Commun.*, 2006, **8**, 348-352. doi:10.1016/j.elecom.2005.12.003.
- 113 D. H. Kim, O. J. Lee, E. Barriau, X. Li, A. M. Caminade, J. P. Majoral, H. Frey and W. Knoll, *J. Nanosci. Nanotechnol.*, 2006, **6**, 3871-3876. doi:10.1166/jnn.2006.669.
- 114 D. S. dos Santos, M. R. Cardoso, F. L. Leite, R. F. Aroca, L. H. C. Mattoso, O. N. Oliveira and C. R. Mendonça, *Langmuir*,

- 2006, **22**, 6177-6180. doi:10.1021/la060399q.
- 115 J. L. Hernandez-Lopez, H. L. Khor, A. M. Caminade, J. P. Majoral, S. Mittler, W. Knoll and D. H. Kim, *Thin Solid Films*, 2008, **516**, 1256-1264. doi:10.1016/j.tsf.2007.05.049.
- 116 D. Lombardo, *Biochem. Res. Int.*, 2014, **2014**. doi:10.1155/2014/837651.
- 117 J. Yuan, D. Han, Y. Zhan, Y. F. Shen, Z. Wang, Q. Zhang and L. Niu, *J. Electroanal. Chem.*, 2007, **599**, 127-135. doi:10.1016/j.jelechem.2006.09.025.
- 118 W. Xu, P. A. Ledin, V. V. Shevchenko and V. V. Tsukruk, *ACS Appl. Mater. Interfaces*, 2015, **7**, 12570-12596. doi:10.1021/acsami.5b01833.
- 119 V. V. Tsukruk, F. Rinderspacher and V. N. Bliznyuk, *Langmuir*, 1997, **13**, 2171-2176. doi:10.1021/la960603h.
- 120 K. Esumi, S. Akiyama and T. Yoshimura, *Langmuir*, 2003, **19**, 7679-7681. doi:10.1021/la034777s.
- 121 K. Yoshida, K. Suwa and J. I. Anzai, *Materials*, 2016, **9**, 425. doi:10.3390/ma9060425.
- 122 Y. Niu, L. Sun and R. M. Crooks, *Macromolecules*, 2003, **36**, 5725-5731. doi:10.1021/ma034276d.
- 123 A. J. Khopade and F. Caruso, *Langmuir*, 2002, **18**, 7669-7676. doi:10.1021/la020251g.
- 124 P. Welch and M. Muthukumar, *Macromolecules*, 1998, **31**, 5892-5897. doi:10.1021/ma980198w.
- 125 J. W. A. van den Berg and A. J. Staverman, *Recl. Des Trav. Chim Des Pays-Bas*, 1972, **91**, 1151-1162. doi:10.1002/recl.19720911002.
- 126 R. Windsor, D. J. Neivandt and P. B. Davies, *Langmuir*, 2001, **17**, 7306-7312. doi:10.1021/la010505i.
- 127 M. S. Johal, B. H. Ozer, J. L. Casson, A. S. John, J. M. Robinson and H. L. Wang, *Langmuir*, 2004, **20**, 2792-2796. doi:10.1021/la0363635.
- 128 A. J. Khopade and F. Caruso, *Nano Lett.*, 2002, **2**, 415-418. doi:10.1021/nl015696o.
- 129 P. J. G. Goulet, D. S. dos Santos, R. A. Alvarez-Puebla, O. N. Oliveira and R. F. Aroca, *Langmuir*, 2005, **21**, 5576-5581. doi:10.1021/la050202e.
- 130 H. Zhang, Y. Fu, D. Wang, L. Wang, Z. Wang and X. Zhang, *Langmuir*, 2003, **19**, 8497-8502. doi:10.1021/la035036u.
- 131 S. Jing, W. Liyan, G. Jian, Y. Xi and Z. Xi, *Chinese Sci. Bull.*, 2005, **50**, 374-376. doi:10.1360/982004-471.
- 132 K. Sato, S. Takahashi and J. I. Anzai, *Anal. Sci.*, 2012, **28**, 929-938. doi:10.2116/analsci.28.929.
- 133 F. Huo, H. Xu, L. Zhang, Y. Fu, Z. Wang and X. Zhang, *Chem. Commun.*, 2003, **3**, 874-875. doi:10.1039/b300405h.
- 134 J. Sun, L. Wang, X. Yu and X. Zhang, *Eur. Polym. J.*, 2005, **41**, 1219-1224. doi:10.1016/j.eurpolymj.2004.12.014.
- Y. Fu, S. Bai, S. Cui, D. Qiu, Z. Wang and X. Zhang, *Macromolecules*, 2002, **35**, 9451-9458. doi:10.1021/ma0207881.
- J. Sun, L. Wang, J. Gao and Z. Wang, *J. Colloid Interface Sci.*, 2005, **287**, 207-212. doi:10.1016/j.jcis.2005.01.068.
- H. Lee, R. Mensire, R. E. Cohen and M. F. Rubner, *Macromolecules*, 2012, **45**, 347-355. doi:10.1021/ma202092w.
- S. Tomita, K. Sato and J. I. Anzai, *J. Colloid Interface Sci.*, 2008, **326**, 35-40. doi:10.1016/j.jcis.2008.06.054.
- C. Park, M. Rhue, M. Im and C. Kim, *Macromol. Res.*, 2007, **15**, 688-692. doi:10.1021/nn700408z.
- K. M. Gattás-Asfura, M. Valdes, E. Celik and C. L. Stabler, *J. Mater. Chem. B*, 2014, **2**, 8208-8219. doi:10.1039/c4tb01241k.
- F. N. Crespilho, V. Zucolotto, O. N. Oliveira and F. C. Nart, *Int. J. Electrochem. Sci.*, 2006, **1**, 194-214.
- Y. Liu, M. L. Bruening, D. E. Bergbreiter and R. M. Crooks, *Angew. Chemie Int. Ed.*, 1997, **36**, 2114-2116. doi:10.1002/anie.199721141.
- M. Zhao, Y. Liu, R. M. Crooks and D. E. Bergbreiter, *J. Am. Chem. Soc.*, 1999, **121**, 923-930. doi:10.1021/ja9825027.
- Y. Jia and J. Li, *Chem. Rev.*, 2015, **115**, 1597-1621. doi:10.1021/cr400559g.
- J. Wang, X. Jia, H. Zhong, Y. Luo, X. Zhao, W. Cao and M. Li, *Chem. Mater.*, 2002, **14**, 2854-2858. doi:10.1021/cm010922g.
- J. Wang, J. Chen, X. Jia, W. Cao and M. Li, *Chem. Commun.*, 2000, **6**, 511-512. doi:10.1039/a909441e.
- Y. Luo, Y. Li, X. Jia, H. Yang, L. Yang, Q. Zhou and Y. Wei, *J. Appl. Polym. Sci.*, 2003, **89**, 1515-1519. doi:10.1002/app.12229.
- H. C. Kolb, M. G. Finn and K. B. Sharpless, *Angew. Chemie Int. Ed.*, 2001, **40**, 2004-2021. doi:10.1002/1521-3773(20010601)40:11<2004::AID-ANIE2004>3.0.CO;2-5.
- E. Lallana, F. Fernandez-Trillo, A. Sousa-Herves, R. Riguera and E. Fernandez-Megia, *Pharm. Res.*, 2012, **29**, 902-921. doi:10.1007/s11095-012-0683-y.
- C. Barner-Kowollik, F. E. D. Prez, P. Espeel, C. J. Hawker, T. Junkers, H. Schlaad and W. V. Camp, *Angew. Chemie Int. Ed.*, 2011, **50**, 60-62. doi:10.1002/anie.201003707.
- C. W. Tornøe, C. Christensen and M. Meldal, *J. Org. Chem.*, 2002, **67**, 3057-3064. doi:10.1021/jo011148j.
- V. V. Rostovtsev, L. G. Green, V. V. Fokin and K. B. Sharpless, *Angew. Chemie Int. Ed.*, 2002, **114**, 2708-2711. doi:10.1002/15213773(20020715)41:14<2596::AID-ANIE2596>3.0.CO;2-4.

- 153 H. Li, Z. Li, L. Wu, Y. Zhang, M. Yu and L. Wei, *Langmuir*, 2013, **29**, 3943-3949. doi:10.1021/la400397q.
- 154 K. M. Gattás-Asfura and C. L. Stabler, *ACS Appl. Mater. Interfaces*, 2013, **5**, 9964-9974. doi:10.1021/am401981g.
- 155 K. M. Gattás-Asfura, N. J. Abuid, I. Labrada and C. L. Stabler, *ACS Biomater. Sci. Eng.*, 2020, **6**, 2641-2651. doi:10.1021/acsbiomaterials.9b01033.
- 156 F. E. Appoh and H. B. Kraatz, *J. Appl. Polym. Sci.*, 2008, **111**, 709-723. doi:10.1002/app.28980.
- 157 D. R. Blasini, S. Flores-Torres, D. M. Smilgies and H. D. Abruña, *Langmuir*, 2006, **22**, 2082-2089. doi:10.1021/la052558w.
- 158 N. B. Pramanik, C. Tian, E. R. Stedronsky and S. L. Regen, *ACS Appl. Polym. Mater.*, 2019, **1**, 141-144. doi:10.1021/acsapm.8b00219.
- 159 O. Crespo-Biel, B. Dordi, D. N. Reinhoudt and J. Huskens, *J. Am. Chem. Soc.*, 2005, **127**, 7594-7600. doi:10.1021/ja051093t.
- 160 B. J. Ravoo, *Dalt. Trans.*, 2008, **12**, 1533-1537. doi:10.1039/b718133g.
- 161 O. Crespo-Biel, B. Dordi, P. Maury, M. Péter, D. N. Reinhoudt and J. Huskens, *Chem. Mater.*, 2006, **18**, 2545-2551. doi:10.1021/cm052796c.
- 162 W. Müller, H. Ringsdorf, E. Rump, G. Wildburg, X. Zhang, L. Angermaier, W. Knoll, M. Liley and J. Spinke, *Science*, 1993, **262**, 1706-1708. doi:10.1126/science.8259513.
- 163 C. Bourdillon, C. Demaille, J. Moiroux and J. M. Savéant JM, *Acc. Chem. Res.*, 1996, **29**, 529-535. doi:10.1021/ar960137n.
- 164 E. Mahon, Z. Mouline, M. Sillion, A. Gilles, M. Pinteala and M. Barboiu, *Chem. Commun.*, 2013, **49**, 3004-3006. doi:10.1039/c3cc41074a.
- 165 S. Hou, J. Wang and C. R. Martin, *J. Am. Chem. Soc.*, 2005, **127**, 8586-8587. doi:10.1021/ja042343t.
- 166 J. I. Anzai, Y. Kobayashi, N. Nakamura, M. Nishimura and T. Hoshi, *Langmuir*, 1999, **15**, 221-226. doi:10.1021/la980743m.
- 167 C. L. Feng, A. M. Caminade, J. P. Majoral and D. Zhang, *J. Mater. Chem.*, 2010, **20**, 1438-1441. doi:10.1039/b927566e.
- 168 C. L. Feng, A. M. Caminade, J. P. Majoral, J. Gu, S. Zhu, H. Su, X. Hu and D. Zhang, *Analyst*, 2010, **135**, 2939-2944. doi:10.1039/c0an00334d.
- 169 H. Moorthy and T. Govindaraju, *ACS Appl. Bio Mater.*, 2021, **4**, 1115-1139. doi:10.1021/acsabm.0c01319.
- 170 J. R. Siqueira, L. Caseli, F. N. Crespilho, V. Zucolotto and O. N. Oliveira, *Biosens. Bioelectron.*, 2010, **25**, 1254-1263. doi:10.1016/j.bios.2009.09.043.
- 171 A. Kawamura and T. Miyata, in *Biomaterials nanoarchitectonics*, ed. M. Ebara, William Andrew, 2016, pp. 157-176.
- 172 S. S. Mark, N. Sandhyarani, C. Zhu, C. Campagnolo and C. A. Batt, *Langmuir*, 2004, **20**, 6808-6817. doi:10.1021/la0495276.
- 173 C. L. Feng, M. Yin, D. Zhang, S. Zhu, A. M. Caminade, J. P. Majoral and K. Müllen, *Macromol. Rapid Commun.*, 2011, **32**, 679-683. doi:10.1002/marc.201000788.
- 174 E. Lojou and P. Bianco, *Bioelectrochemistry*, 2006, **69**, 237-247. doi:10.1016/j.bioelechem.2006.03.028
- 175 H. C. Yoon and H. S. Kim, *Anal. Chem.*, 2000, **72**, 922-926. doi:10.1021/ac991299a.
- 176 L. Shen and N. Hu, *Biomacromolecules*, 2005, **6**, 1475-1483. doi:10.1021/bm049248x.
- 177 H. Zhang and N. Hu, *Biosens. Bioelectron.*, 2007, **23**, 393-399. doi:10.1016/j.bios.2007.04.018.
- 178 Y. Zhu, H. Zhu, X. Yang, L. Xu and C. Li, *Electroanalysis*, 2007, **19**, 698-703. doi:10.1002/elan.200603802.
- 179 L. Tang, Y. Zhu, L. Xu, X. Yang and C. Li, *Electroanalysis*, 2007, **19**, 1677-1682. doi:10.1002/elan.200703904.
- 180 J. R. Siqueira, M. H. Abouzar, A. Poghossian, V. Zucolotto, O. N. Oliveira and M. J. Schöning, *Biosens. Bioelectron.*, 2009, **25**, 497-501. doi:10.1016/j.bios.2009.07.007.
- 181 S. Svenson and D. A. Tomalia, *Adv. Drug Deliv. Rev.*, 2005, **57**, 2106-2129. doi:10.1016/j.addr.2012.09.030.
- 182 S. H. Wang, X. Shi, M. V. Antwerp, Z. Cao, S. D. Swanson, X. Bi and J. R. Baker, *Adv. Funct. Mater.*, 2007, **17**, 3043-3050. doi:10.1002/adfm.200601139.
- 183 P. Garrigue, J. Tang, L. Ding, A. Bouhleb, A. Tintaru, E. Laurini, Y. Huang, Z. Lyu, M. Zhang, S. Fernandez, et al., *Proc. Natl. Acad. Sci.*, 2018, **115**, 11454-11459. doi:10.1073/pnas.1812938115.
- 184 L. Ding, Z. Lyu, A. Tintaru, E. Laurini, D. Marson, B. Louis, A. Bouhleb, L. Balasse, S. Fernandez, P. Garrigue, et al., *Chem. Commun.*, 2020, **56**, 301-304. doi:10.1039/c9cc07750b.
- 185 M. A. Mintzer and E. E. Simanek, *Chem. Rev.*, 2009, **109**, 259-302. doi:10.1021/cr800409e.
- 186 J. M. Silva, S. G. Caridade, R. R. Costa, N. M. Alves, T. Groth, C. Picart, R. L. Reis and J. F. Mano, *Langmuir*, 2015, **31**, 11318-11328. doi:10.1021/acs.langmuir.5b02478.
- 187 E. Ahn, H. Gaiji, T. Kim, M. Abderrabba, H. W. Lee and B. S. Kim, *J. Memb. Sci.*, 2019, **585**, 191-198. doi:10.1016/j.memsci.2019.05.035.
- 188 Z. Gui, B. Du, J. Qian, Q. An and Q. Zhao, *J. Colloid Interface Sci.*, 2011, **353**, 98-106. doi:10.1016/j.jcis.2010.09.026.
- 189 A. Zhuk, S. Pavlkhina and S. A. Sukhishvili, *Langmuir*, 2009, **25**, 14025-14029. doi:10.1021/la901478v.

Journal Name	ARTICLE
190 Z. Zhu and S. A. Sukhishvili, <i>ACS Nano</i> , 2009, <b>3</b> , 3595-3605. doi:10.1021/nn900655z.	209 U. Akiba, D. Minaki and J. I. Anzai, <i>Polymers</i> , 2017, <b>9</b> , 553. doi:10.3390/polym9110553.
191 B. G. De Geest, A. M. Jonas, J. Demeester and S. C. De Smedt, <i>Langmuir</i> , 2006, <b>22</b> , 5070-5074. doi:10.1021/la053368o.	210 Y. Jia and J. Li, <i>Langmuir</i> , 2019, <b>35</b> , 8557-8564. doi:10.1021/acs.langmuir.8b04319.
192 D. Bruen, P. P. Campos, M. Ferreira, D. Diamond, C. Delaney and L. Florea, <i>ACS Appl. Polym. Mater.</i> , 2019, <b>1</b> , 990-996. doi:10.1021/acsapm.9b00017.	211 S. Tomita, K. Sato and J. I. Anzai, <i>Mater. Sci. Eng. C</i> , 2009, <b>29</b> , 2024-2028. doi:10.1016/j.msec.2009.03.019.
193 H. Sato, Y. Takano, K. Sato and J. I. Anzai, <i>J. Colloid Interface Sci.</i> , 2009, <b>333</b> , 141-144. doi:10.1016/j.jcis.2008.12.071.	212 A. J. Khopade and F. Caruso, <i>Biomacromolecules</i> , 2002, <b>3</b> , 1154-1162. doi:10.1021/bm025562k.
194 S. Takahashi, Y. Aikawa, T. Kudo, T. Ono, Y. Kashiwagi and J. I. Anzai, <i>Colloid Polym. Sci.</i> , 2014, <b>292</b> , 771-776. doi:10.1007/s00396-014-3169-0.	213 A. J. Khopade and F. Caruso, <i>Langmuir</i> , 2003, <b>19</b> , 6219-6225. doi:10.1021/la030016d.
195 G. Rydzek, Q. Ji, M. Li, P. Schaaf, J. P. Hill, F. Boulmedais and K. Ariga, <i>Nano Today</i> , 2015, <b>10</b> , 138-167. doi:10.1016/j.nantod.2015.02.008.	214 B. S. Kim, O. V. Lebedeva, D. H. Kim, A. M. Caminade, J. P. Majoral, W. Knoll and O. I. Vinogradova, <i>Langmuir</i> , 2005, <b>21</b> , 7200-7206. doi:10.1021/la0504208.
196 F. Sato and J. I. Anzai, <i>Mater. Sci. Eng. C</i> , 2017, <b>72</b> , 118-122. doi:10.1016/j.msec.2016.11.061.	215 B. S. Kim, O. V. Lebedeva, K. Koynov, H. Gong, A. M. Caminade, J. P. Majoral and O. I. Vinogradova, <i>Macromolecules</i> , 2006, <b>39</b> , 5479-5483. doi:10.1021/ma060698m.
197 K. Suwa, M. Nagasaka, S. Niina, Y. Egawa, T. Seki and J. I. Anzai, <i>Colloid Polym. Sci.</i> , 2015, <b>293</b> , 1043-1048. doi:10.1007/s00396-014-3490-7.	216 B. S. Kim, O. V. Lebedeva, M. K. Park, W. Knoll, A. M. Caminade, J. P. Majoral and O. I. Vinogradova, <i>Polymer</i> , 2010, <b>51</b> , 4525-4529. doi:10.1016/j.polymer.2010.08.005.
198 K. Suwa, K. Sato and J. I. Anzai, <i>Colloid Polym. Sci.</i> , 2015, <b>293</b> , 2713-2718. doi:10.1007/s00396-015-3722-5.	217 S. Mignani, X. Shi, M. Zablocka and J. P. Majoral, <i>Biomacromolecules</i> , 2021, <b>22</b> , 262-274. doi:10.1021/acs.biomac.0c01645.
199 K. Sato, K. Awaji, M. Ito and J. I. Anzai, <i>Colloid Polym. Sci.</i> , 2017, <b>295</b> , 877-882. doi:10.1007/s00396-017-4073-1.	218 A. Sousa-Herves, E. Fernandez-Megia and R. Riguera, <i>Chem. Commun</i> , 2008, <b>27</b> , 3136-3138. doi:10.1039/b805208e.
200 Q. Jiao, Z. Yi, Y. Chen and F. Xi, <i>Polymer</i> , 2008, <b>49</b> , 1520-1526. doi:10.1016/j.polymer.2008.01.064.	219 M. Fernandez-Villamarin, A. Sousa-Herves, S. Porto, N. Guldris, J. Martínez-Costas, R. Riguera and E. Fernandez-Megia, <i>Polym. Chem.</i> , 2017, <b>8</b> , 2528-2537. doi:10.1039/c7py00304h.
201 Y. Wang, Q. An, Y. Zhou, Y. Niu, R. Akram, Y. Zhang and F. Shi, <i>J. Mater. Chem. B</i> , 2015, <b>3</b> , 562-569. doi:10.1039/c4tb01688b.	220 S. P. Amaral, M. H. Tawara, M. Fernandez-Villamarin, E. Borrajo, J. Martínez-Costas, A. Vidal, R. Riguera and E. Fernandez-Megia, <i>Angew. Chemie Int. Ed.</i> , 2018, <b>57</b> , 5273-5277. doi:10.1002/anie.201712244.
202 X. Liu, K. Zhao, C. Jiang, Y. Wang, L. Shao, Y. Zhang and F. Shi, <i>Soft Matter</i> , 2015, <b>11</b> , 5748-5753. doi:10.1039/c5sm01055a.	221 G. D. Zhang, A. Harada, N. Nishiyama, D. L. Jiang, H. Koyama, T. Aida and K. Kataoka, <i>J. Control Release</i> , 2003, <b>93</b> , 141-150. doi:10.1016/j.jconrel.2003.05.002.
203 F. Ji, L. You, L. Wang, Z. Liu, Y. Zhang and S. Lv, <i>Ind. Eng. Chem. Res.</i> , 2016, <b>55</b> , 10664-10670. doi:10.1021/acs.iecr.6b02080.	222 N. Nishiyama, H. R. Stapert, G. D. Zhang, D. Takasu, D. L. Jiang, T. Nagano, T. Aida and K. Kataoka, <i>Bioconju. Chem.</i> , 2003, <b>14</b> , 58-66. doi:10.1021/bc025597h.
204 T. Huang, Q. An, X. Luan, Q. Zhang and Y. Zhang, <i>Nanoscale</i> , 2016, <b>8</b> , 2003-2010. doi:10.1039/c5nr08129g.	223 K. Karthikeyan, A. Babu, S. J. Kim, R. Murugesan and K. Jeyasubramanian, <i>Cancer Nano</i> , 2011, <b>2</b> , 95-103. doi:10.1007/s12645-011-0019-3.
205 H. Du, Y. Zhang and S. Lv, <i>Colloid Polym. Sci.</i> , 2017, <b>295</b> , 317-325. doi:10.1007/s00396-016-3990-8.	224 Y. Yan, J. Zhang, L. Ren and C. Tang, <i>Chem. Soc. Rev.</i> , 2016, <b>45</b> , 5232-5263. doi:10.1039/c6cs00026f.
206 Y. Zhang, Q. An, W. Tong, H. Li, Z. Ma, Y. Zhou, T. Huang and Y. Zhang, <i>Small</i> , 2018, <b>14</b> , 1802136. doi:10.1002/sml.201802136.	225 J. Zhao, W. Wu, J. Sun and S. Guo, <i>Chem. Soc. Rev.</i> , 2013, <b>42</b> , 5323-5351. doi:10.1039/c3cs35531d.
207 M. L. Moraes, M. S. Baptista, R. Itri, V. Zucolotto, O. N. Oliveira, <i>Mater. Sci. Eng. C</i> , 2008, <b>28</b> , 467-471. doi:10.1016/j.msec.2007.04.017.	226 K. E. Borbas and D. Lahaye, in <i>Anticancer therapeutics</i> , ed. S. Missailidis, John Wiley & Sons, UK, 2008, pp. 187-222.
208 H. Lin, W. Xiao, S. Y. Qin, S. X. Cheng and X. Z. Zhang, <i>Polym. Chem.</i> , 2014, <b>5</b> , 4437-4440. doi:10.1039/c4py00564c.	

- 227 P. Agostinis, K. Berg, K. A. Cengel, T. H. Foster, A. W. Girotti, S. O. Gollnick, S. M. Hahn, M. R. Hamblin, A. Juzeniene, D. Kessel, M. Korbelik, et al., *CA Cancer J. Clin.*, 2011, **61**, 250-281. doi:10.3322/caac.20114.
- 228 M. R. Hamblin, *Photochem Photobiol.*, 2020, **96**, 506-516. doi:10.1111/php.13190.
- 229 K. J. Son, H. J. Yoon, J. H. Kim, W. D. Jang, Y. Lee and W. G. Koh, *Angew. Chemie Int. Ed.*, 2011, **50**, 11968-11971. doi:10.1002/anie.201102658.
- 230 N. Peng, H. Yu, Z. Wang, Y. Zhang, K. Deng, J. Li, L. Lu, T. Zou, Y. Liu and S. Huang, *Mater. Sci. Eng. C*, 2019, **98**, 737-745. doi:10.1016/j.msec.2018.12.111.
- 231 V. Leiro, J. P. Garcia, H. Tomás, A. P. Pêgo, *Bioconjug. Chem.*, 2015, **26**, 1182-1197. doi:10.1021/bc5006224.
- 232 S. Jiang, Y. Chen, G. Duan, C. Mei, A. Greiner and S. Agarwal, *Polym. Chem.*, 2018, **9**, 2685-2720. doi:10.1039/c8py00378e.
- 233 X. Feng, J. Li, X. Zhang, T. Liu, J. Ding and X. Chen, *J. Control Release*, 2019, **302**, 19-41. doi:10.1016/j.jconrel.2019.03.020.
- 234 S. Xiao, Q. Peng, Y. Yang, Y. Tao, Y. Zhou, W. Xu and X. Shi, *ACS Appl. Bio Mater.*, 2019, **3**, 346-357. doi:10.1021/acsabm.9b00848.
- 235 K. Ramalingam, R. Castro, P. Pires, X. Shi, J. Rodrigues, S. Xiao and H. Tomás, *RSC Adv.*, 2016, **6**, 97116-97128. doi:10.1039/c6ra22444j.
- 236 W. Chen, W. Li, K. Xu, M. Li, L. Dai, X. Shen, Y. Hu and K. Cai, *J. Biomed. Mater. Res. - Part A*, 2018, **106**, 706-717. doi:10.1002/jbm.a.36273.
- 237 M. V. Walter and M. Malkoch, *Chem. Soc. Rev.*, 2012, **41**, 4593-4609. doi:10.1039/c2cs35062a.
- 238 Z. Lyu, L. Ding, A. Tintaru and L. Peng, *Acc. Chem. Res.*, 2020, **53**, 2936-2949. doi:10.1021/acs.accounts.0c00589.

This review provides a comprehensive and critical overview of the supramolecular dendrimer-containing multifunctional layer-by-layer nanoassemblies driven by a multitude of intermolecular interactions for biological and biomedical applications.

